A COMPUTER REPRESENTATION OF A BRUSHLESS EXCITATION SYSTEM

BY

MD. ABDUS SATTAR

A THESIS

SUBMITTED TO THE DEPARTMENT OF ELECTRICAL AND ELECTRONIC ENGINEEING, BUET IN PARTIAL FULFILMENT OF THE REQUIREMENTS FOR THE DEGREE OF MASTER OF SCIENCE IN ENGINEERING

DEPARTMENT OF ELECTRICAL AND ELECTRONIC ENGINEERING

BANGLADESH UNIVERSITY OF ENGINEERING AND TECHNOLOGY, DHAKA

DECEMBER, 1990.

Accepted as satisfactory in the partial fulfilment of the requirements for the degree of Master of Science in Engineering (Electrical and Electronic).

BOARD OF EXAMINER

1. ---------31/12/90--------- Chairman
(Dr. S. M. Lutful Kabir) (Supervisor)
Assistant professor,
Department of Electrical and
Electronic Engineering, BUET
Dhaka, Bangladesh.

2. ---------- Member
(Dr. S. F. Rahman) (Ex- officio)
Professor and Head,
Department of Electrical and
Electronic Engineering, BUET
Dhaka, Bangladesh.

3. ---------- Member
(Dr. Md. Mujibur Rahman)
Professor and Dean,
Faculty of Electrical and
Electronic Engineering, BUET
Dhaka, Bangladesh.

4. ---------- Member
(Dr. Mohammed Ali Chowdhury)
Assistant professor,
Department of Electrical and
Electronic Engineering, BUET
Dhaka, Bangladesh.

5. ---------- Member
(Dr. Nazrul Islam) (External)
Ex. Rector, BPATC,
House No. - 61, Road No. - 17,
Block - E, Banani, Dhaka, Bangladesh.

DECLARATION

No portion of this work has been submitted to any other university or similar institution for the award of any degree.

Countersigned by

31/12/90

(Dr. S. M. Lutful Kabir)
Supervisor

Md. Abdus Sattar

(Md. Abdus Sattar)

CONTENTS

Chapter 3
EXCITATION TO AN ALTERNATOR WITH NO LOAD

Chapter 4
EXCITATION TO AN ALTERNATOR WITH LOAD

Chapter 5
CONCLUSIONS AND DISCUSSIONS

ACKNOWLEDGEMENT

It is a matter of great pleasure on the part of the author to acknowledge his gratitude and profound respect to his supervisor, Dr. S. M. Lutful Kabir, Assistant professor, Department of Electrical and Electronic Engineering, Bangladesh University of Engineering and Technology, BUET for his valuable guidance, constant encouragement and whole hearted supervision throughout the progress of the work.

The author also wishes to express his thanks and gratitude to Dr. S. F. Rahman, Professor and Head, Department of Electrical and Electronic Engineering, BUET for his encouragement and allout support for successful completion of the work.

The author also acknowledge his gratitude to Dr. Md. Mujibur Rahman, Professor and Dean, Faculty of Electrical and Electronic Engineering and Dr. Mohammed Ali Chowdhury, Assistant professor, Department of Electrical and Electronic Engineering, BUET for their valiable suggestions and encouragement.

Finally, the author is also indebted to Mr. A. Towhid, Executive Director, Mr. Golam Sarwar, Programmar and all the staff of IBCS-PRIMAX Software (Bangladesh) Ltd. for their co-operation.

Abstract

A computer model of brushless excitation system for large alternators has been developed. The model is based on detail understanding of principle of its operation under varying terminal conditions. The exciter-alternator is simulated by five-winding representation as suggested by Canay and the rectifier unit is modelled on the basis of analytical expressions representing different mode of operations. Each module of the brushless excitation system has been joined together to form a complete model which can easily be rearranged to simulate a particular condition.

Responses of brushless excitation system under both transient and steady state condition have been simulated. The result of the developed model is compared with test response and found to have good agreement. The outcome of the model is also judged against IEEE model and the model developed is ranked to be a superior one. In this respect the shortcomings of the IEEE model are also pointed out. The work presented in this thesis would form a basis of modelling alternators having brushless excitation systems.

List of Symbols

X_a = Armature reactance.

R_a = Armature resistance.

X_{md} = Direct axis magnetising reactance.

X_{kd} = Direct axis damper reactance.

R_{kd} = Direct axis damper resistance.

X_f = Field reactance.

R_f = Field resistance.

X_{mq} = Quadrature axis magnetising reactance.

X_{kq} = Quadratute axis damper reactance.

R_{kq} = Quadrature axis damper resistance.

u_d = Direct axis voltage.

u_q = Quadrature axis voltage.

Φ's = Flux terms.

Y's = Admittance terms.

X's = Impedance terms.

p = Derivative (d/dt).

w_o = Synchronous speed.

X_c = Commutating reactance.

V_E = Exciter phase voltage behind commutating reactance.

E_d = Theoretical rectifier output voltage under load.

ΔE_d = Rectifier voltage drop due to commutation.

E_{do} = Theoretical rectifier output voltage at no load.

u = Commutating angle, radians or degree.

α = Delay angle, radians or degree.

I_n = Normalised current.

F_{ex} = Rectifier loading factor.

A1 = Real component of the phase current.

B1 = Reactive component of the phase current.

I_{de} = Direct axis component of the alternator current.

I_{qe} = Quadrature axis component of the alternator current.

I_d = Direct axis component of the alternator current considering delay angle.

I_q = Quadrature axis component of the alternator current considering delay angle.

E_{fd} = Field voltage of the main alternator.

I_{fd} = Load current.

I_{fg} = Field current of the main alternator.

K_d = Feedback factor.

Chapter 1

INTRODUCTION

1.1 General

When the response of a synchronous machine in power system stability studies is to be accurately predicted, it is essential that its excitation system be modelled in sufficient detail. The required model must be suitable for representing the actual excitation equipment performance for large, severe disturbances as well as for small perturbations.

Considerable attention has been given in the literature to the excitation system and its role in improving power system stability [1-3]. Early investigators realized that the so-called "steady-state" power limits of power networks could be increased using the available high-gain continuous acting voltage regulator [2]. It was also recognised that the voltage regulator gain requirement was different at no load conditions from that needed for good performance under load [4]. Following extensive investigation on excitation control, success has been achieved in improving power system dynamic performance. With the advent of fast-acting excitation system, the machines are now-a-days operated with large rotor angle [5]. On the otherhand, large machines having low interia, are prone to instablility when operated at large rotor angle. As a result, accurate prediction of excitation requirement is inevitable before designing fast-acting automatic voltage regulator which controls excitation to

the machine.

1.2 Simplified view of excitation system

Let us now consider the physical configuration of components used for excitation systems. Figure 1.1 shows in block form the arrangement of a system.

In many systems the exciter is a dc generator driven by either the steam turbine on the same shaft as the generator or an induction motor. Solid-state systems consisting of some form of rectifier or thyristor system supplied from ac bus or from alternator-exciter are increasing in use.

The voltage regulator is the intelligence of the system and controls the output of the exciter so that the generated voltage and reactive power change in the desired way. In earlier systems the "voltage regulator" was entirely manual. In most modern systems the voltage regulator is a controller that senses the generator output voltage and then initiates corrective action by changing the exciter control in the desired direction.

1.3 Types of Excitation systems

Different types of excitation system are in use with synchronous generators. The dc power required to excite the field of a generator varies as its size increases. On the basis of

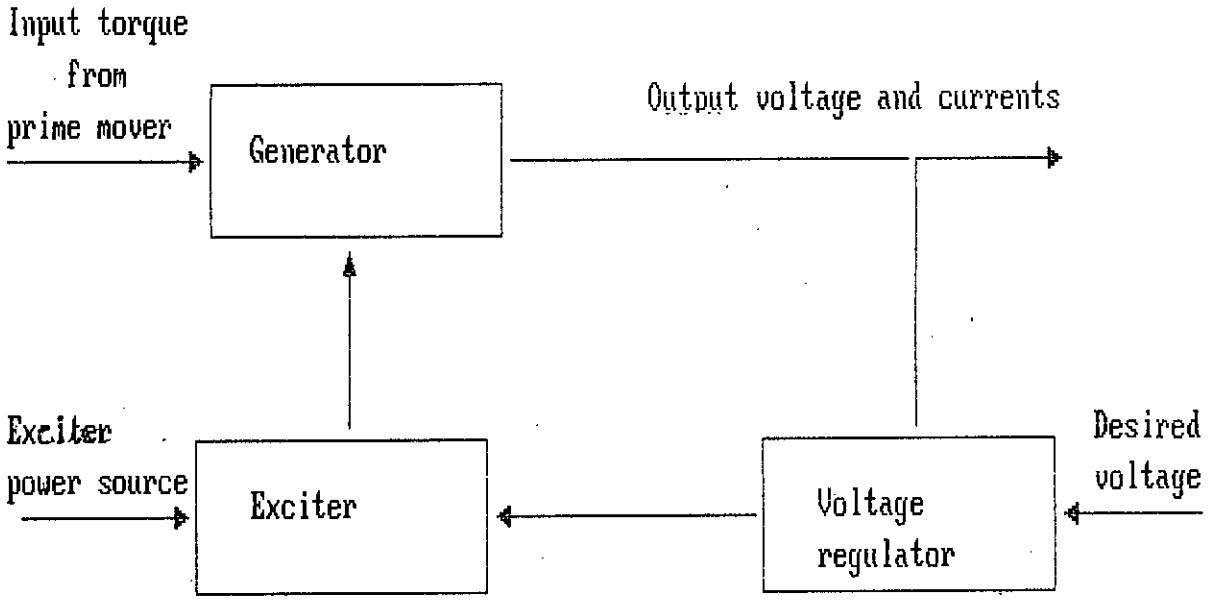

Fig 1.1 Arrangement of exciter components.

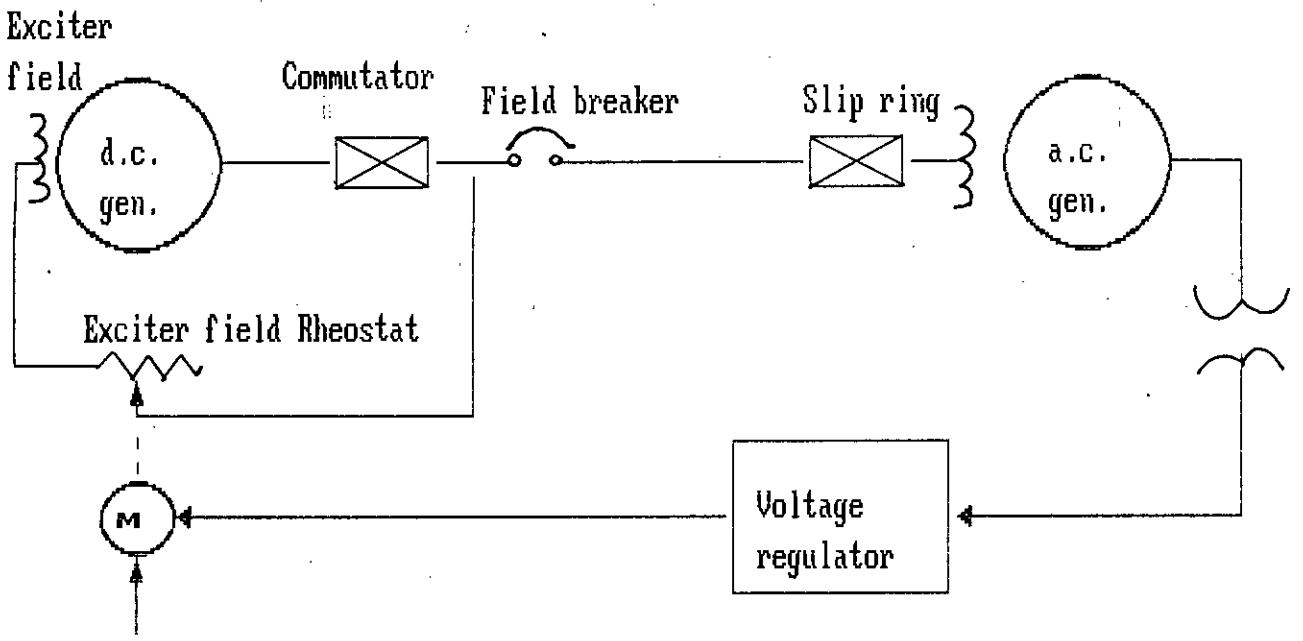

Fig 1.2 Main exciter with rheostat control.

excitation power source, mainly three types of excitation systems are identified.

1.3.1 Primitive Systems

First let us consider systems that can be classified in a general way as "slow response" systems. Figure 1.2 shows one arrangement consisting of main exciter with manual or automatic control of the field. The exciter is essentially a dc generator, the field of which is controlled by a rheostat according to the response of the voltage regulator. One such rheostatic device is described in reference [6].

The next level of complication in excitation systems is the main exciter and pilot exciter system shown in figure 1.3. This system has much faster response than the self- excited main exciter, because the exciter field control is independent of exciter output voltage. Control is achieved in as much the same way as for the self-excited case.

The systems described are examples of older systems that offer little promise for fast system response because of inherent friction, backlash and lack of sensitivity [7].

1.3.2 Alternator rectifier excitation system

With the advent of solid-state technology and availability of reliable high-current rectifiers, another type of system became feasible. In this system the exciter is an ac generator, the output of which is rectified to provide the dc current required by the generator field. In this system the alternator output is rectified and connected to generator field by means of slip rings. The control circuitry for these units is also solid-state in most cases and the overall response is quite fast [8].

1.3.3 Brushless Excitation System

As the available ratings of turbine-generators have increased, the problems of supplying the dc field excitation (amounting 4000 amp or more in the larger units [9]) became progressively more difficult. The excitation systems discussed in section 1.3.1 and 1.3.2 supply dc power to the alternator field through brushes and slip rings. Cooling and maintenance problems are inevitably associated with slip rings, commutators and brushes. A unique excitation system is now being used to eliminate sliding contacts and brushes, thus named `brushless` excitation system [10].

A schematic diagram of the brushless excitation system is given in figure 1.4. At the heart of the system are the diode

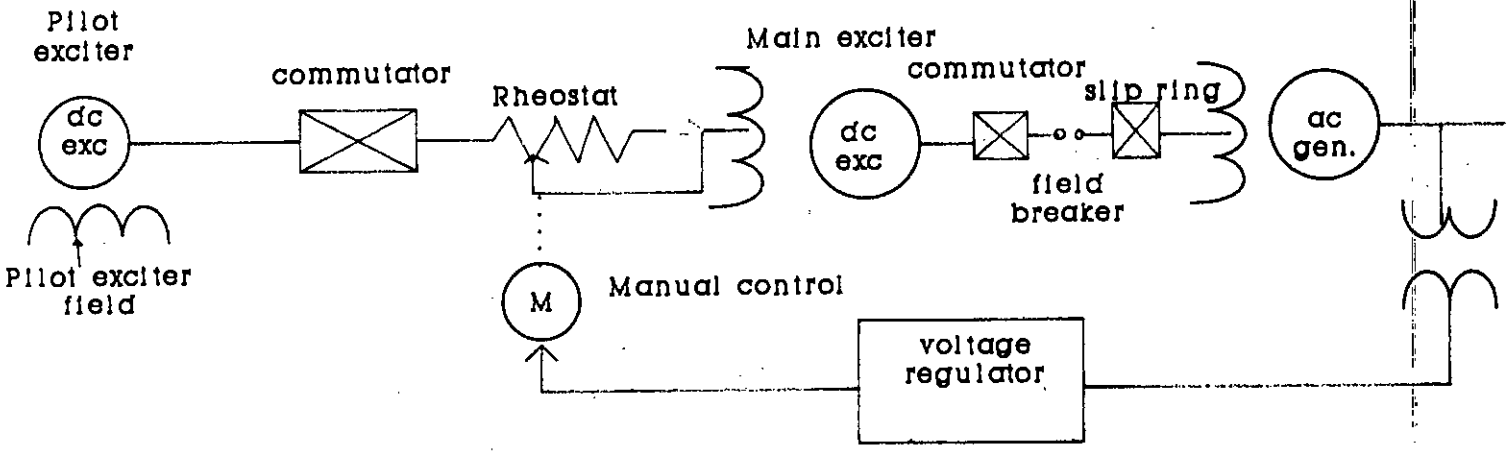

Fig. 1.3 Main exciter and pilot exciter system.

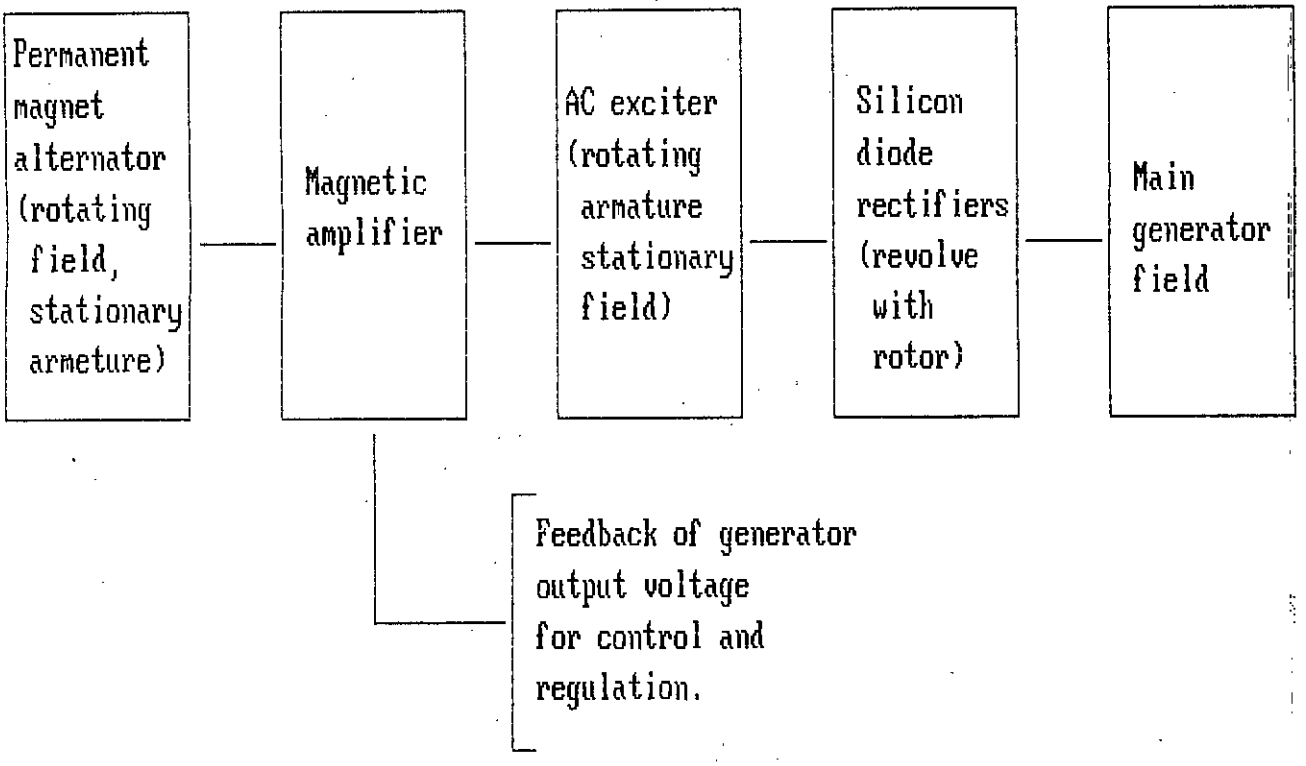

Fig 1.4 A block diagram of brushless excitation system.

rectifiers which are mounted on the same shaft as the generator field and which furnish dc excitation directly to the field. An ac exciter with a rotating armature feeds power along the shaft to the revolving rectifiers. The stationary field of the ac exciter is fed through a magnetic amplifier which controls and regulates the output voltage of the main generator. To make the system self contained and free of sliding contacts, the excitation power for the magnetic amplifier is obtained from the stationary armature of a small permanent-magnet alternator which is also driven from the main shaft. Brushless excitation systems of this type have previously been used in aircraft voltage regulators [11]. Selenium rectifiers were first tried at 3,000 rpm to furnish the d-c power excitation requirement for large generators, but their inability to do so has delayed the application in the electrical utility industry. However, silicon diode rectifiers have since been tested and found to be ideal for this application [12].

It should be noted that in brushless excitation system it is impossible to monitor any of the generator field quantities directly since these components are all moving with the rotor and no slip rings are used. The response of the system is improved by designing the alternator for operation at frequencies higher than that of the main generator. Recent systems [13] have used 420-HZ and 300-HZ alternators for this

reason and provided excellent response characteristics.

1.4 Modelling Brushless Excitation System

The increasing use of rotating-rectifier type brushless excitation system sharpens the need for developing a clear understanding of the behaviour of the brushless excitation system, including the voltage regulator is required, in terms of commonly known machine and system parameters. Such understanding enables predicting the performance of such systems both in the steady state and transient state, and permits determining how the various system characteristics affect performance.

Although a large body of literature exists both on the theory and performance of rectifiers [14-16], relatively little is available about the performance of ac machines supplying rectifier loads, of rectifiers supplied from ac generators, and of synchronous generators deriving their field power from exciter-rectifier systems. Existing published literature on brushless generators and systems generally is confined to a general description of the machine or to some special aspect of system operations, although Ferguson et al [17] and Shilling [18] explore certain special phases of brushless exciter performance.

A IEEE committee report on Excitation system models [19] has

provided a reference for manufactures, owners and system analyst since 1968. It established a common nomenclature, presented mathematical models for excitation system then in common use and defined parameters for those models. An extension of the work was presented in 1981 [20]. It provides models for new types of excitation equipment not covered previously as well as improved models for older equipment. The IEEE model for brushless excitation system has to be investigated because its representation seems to be incomplete.

1.5 Scope of the present work

The present work concern with development of computer model for brushless excitation system. The work starts with establishing a clear understanding of operating principle of brushless excitation system. On the basis of established principle modular representation of exciter-alternator, rectifier, main alternator and loads are to be produced. The alternators involved will be modelled using Park's two axis theory [21] and on the basis of Canay's equivalent circuit representation [22]. The parameters of the machines are obtained from 3-phase short circuit test. The rectifier will be modelled for different mode of its operation individually.

The developed model would be tested against test results and

IEEE model for brushless excitation system. An investigation of influence of machine parameters on system response will be carried out. Further transient and steady-state responses under varying terminal conditions will also be studies. The present work is aimed at developing an accurate universal model for brushless excitation system to be used in power system stability studies.

Chapter 2

MATHEMATICAL MODEL FOR BRUSHLESS EXCITATION SYSTEM

2.1 Introduction

As explained in the previous chapter, a brushless excitation system is essentially an alternator whose output is rectified to supply the d.c. power into the exciter of main alternator. Since all the components are responsible in determining the characteristics of the brushless excitation system, each has to be modelled precisely to produce a composite representation of the excitation system. The representation of alternator has widely been considered previously [23-26], whilst that of rectification process involved in the brushless excitation system has not yet been well-established. The rectifiers undergo four distinct mode of operation as the input voltage and output current varies. The present study investigates the representation of rectifier in detail. The representation is then completed by including the two-axis alternator model. First, the analysis of alternator model is presented.

2.2 Modelling of the alternator at the exciter input

Modelling alternator has become an important subject for power system analyser. Accurate modelling depends on representing the machine by a proper equivalent circuit and the inclusion of various non-linear effects precisely [26]. But this inclusion makes a model complex. The complexity, in most cases, is avoided

in order to minimise computation time. Therefore, a compromise is always sought.

An alternator, in its two axis representation is expressed as five winding machine [27]. D-axis stator, field and d-axis damper winding constitute the direct axis representation, whilst q-axis stator and damper winding are the components of the quadrature axis representation. Such an arrangement is depicted in figure 2.1. To express the two axis machine mathematically, let us consider the direct and quadrature axis voltages u_d and u_q separately as given by :

$$u_d = p\Phi_d + w\Phi_q + R_a i_d \qquad (2.1)$$

$$u_q = p\Phi_q - w\Phi_d + R_a i_q \qquad (2.2)$$

The term $w\Phi_q$ is the voltage induced in the direct axis by virtue of the flux which is centered on the q-axis, where 'w' is the angular velocity of the machine. This may be considered constant and assumed to be equal to synchronous speed w_o, because the voltage variation due to change in speed can be neglected in the present analysis.

The voltage equations of the other rotor circuits are given by :

field ; $u_f = p\Phi_f + R_f i_f \qquad (2.3)$

d-damper ; $0 = p\Phi_{kd} + R_{kd} i_{kd} \qquad (2.4)$

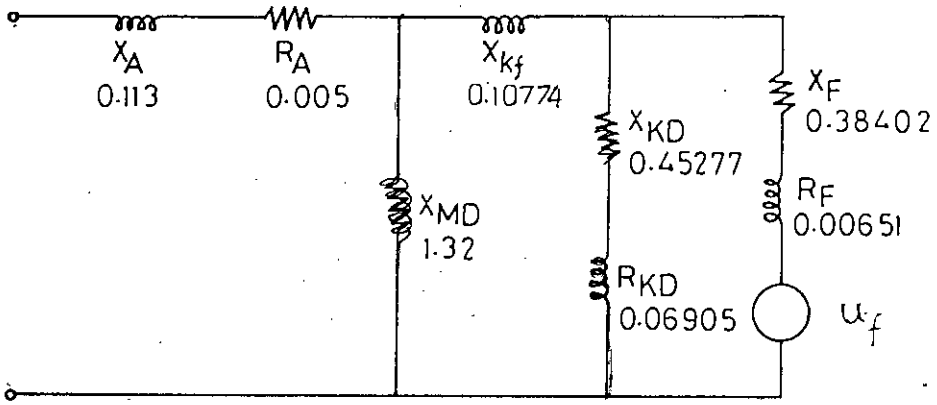

(a) Direct axis

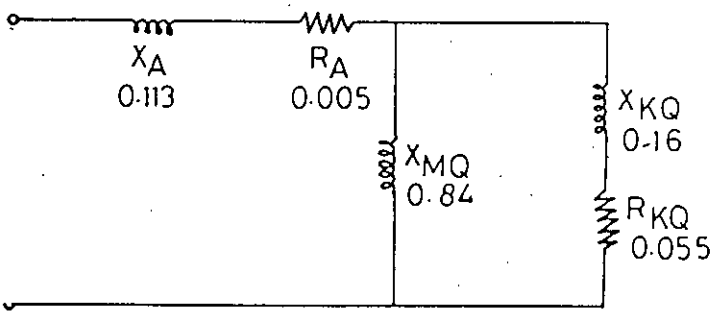

(b) Quadature axis

Fig. 2.1 : Equivalent circuit of d q axis model of the exciter alternator

q-damper ; $0 = p\Phi_{kq} + R_{kq}i_{kq}$ (2.5)

Equations (2.1) to (2.5) can be re-arranged as follows :

$$p\Phi_d = u_d - w_o\Phi_q - R_a i_d \quad (2.6)$$

$$p\Phi_q = u_q + w_o\Phi_d - R_a i_q \quad (2.7)$$

$$p\Phi_f = u_f - R_f i_f \quad (2.8)$$

$$p\Phi_{kd} = -R_{kd} i_{kd} \quad (2.9)$$

$$p\Phi_{kq} = -R_{kq} i_{kq} \quad (2.10)$$

$p\Phi_d$ and $p\Phi_q$ terms in the equations give the decaying dc component in the fluxes and consequently, in currents, following a disturbance. Since only ac components are of much interest, the $p\Phi_d$ and $p\Phi_q$ terms are often omitted from the equations for the sake of simplicity [27]. So, only three equations describing 'p' terms (equations 2.8 to 2.10) are of our concern. The currents in these equations can be related to fluxes in two steps as described below :

First, the relationship between fluxes and currents are expressed as :

d- axis :

$$\begin{bmatrix} w_o\Phi_d \\ w_o\Phi_f \\ w_o\Phi_{kd} \end{bmatrix} = \begin{bmatrix} X_{md} + X_a & X_{md} & X_{md} \\ X_{md} & X_{md}+X_f+X_{kf} & X_{md}+X_{kf} \\ X_{md} & X_{md}+X_{kf} & X_{md}+X_{kd}+X_{kf} \end{bmatrix} \begin{bmatrix} i_d \\ i_f \\ i_{kd} \end{bmatrix} \quad (2.11)$$

q- axis :

$$\begin{bmatrix} w_o\Phi_q \\ w_o\Phi_{kq} \end{bmatrix} = \begin{bmatrix} X_{mq} + X_a & X_{mq} \\ X_{mq} & X_{mq} + X_{kq} \end{bmatrix} \begin{bmatrix} i_q \\ i_{kq} \end{bmatrix} \quad (2.12)$$

where X's are the reactances of the machine.

Secondly, the required relationships of currents in terms of fluxes can be obtained by inverting the reactance matrix of the equation 2.11 and 2.12 . They are :

d- axis :

$$\begin{bmatrix} i_d \\ i_f \\ i_{kd} \end{bmatrix} = \begin{bmatrix} Y_d\,(1,1) & Y_d\,(1,2) & Y_d\,(1,3) \\ Y_d\,(2,1) & Y_d\,(2,2) & Y_d\,(2,3) \\ Y_d\,(3,1) & Y_d\,(3,2) & Y_d\,(3,3) \end{bmatrix} \begin{bmatrix} w_o\Phi_d \\ w_o\Phi_f \\ w_o\Phi_{kd} \end{bmatrix} \quad (2.13)$$

q- axis :

$$\begin{bmatrix} i_q \\ i_{kq} \end{bmatrix} = \begin{bmatrix} Y_q(1,1) & Y_q(1,2) \\ Y_q(2,1) & Y_q(2,2) \end{bmatrix} \begin{bmatrix} w_o\Phi_q \\ w_o\Phi_{kq} \end{bmatrix} \qquad (2.14)$$

Replacing all the current terms of equations 2.8, 2.9 and 2.10 in terms of fluxes, the relationship between rate of change of fluxes with fluxes themselves can be expressed in the form :

$$\dot{[X]} = [A][X] + [B]$$

The final form is :

$$\begin{bmatrix} \dot{w_o\Phi_f} \\ \dot{w_o\Phi_{kd}} \\ \dot{w_o\Phi_{kq}} \end{bmatrix} = \begin{bmatrix} A(1,1) & A(1,2) & A(1,3) & 0 & 0 \\ A(2,1) & A(2,2) & A(2,3) & 0 & 0 \\ 0 & 0 & 0 & A(3,4) & A(3,5) \end{bmatrix} \begin{bmatrix} w_o\Phi_d \\ w_o\Phi_f \\ w_o\Phi_{kd} \\ w_o\Phi_q \\ w_o\Phi_{kq} \end{bmatrix} + \begin{bmatrix} u_f \\ 0 \\ 0 \end{bmatrix}$$

$\dot{[X]}$ $[A]$ $[X]$ $[B]$

(2.15)

where the elements of A-matrix are function of 'Y' terms and R_a.

The change of fluxes are calculated from the equation 2.15 using Runge-Kutta method and new value of Φ_f, Φ_{kd} and Φ_{kq} are then obtained. Once the new value of fluxes are known, the present value of i_f can be obtained from the following relationship.

$$i_f = Y_d(2,1)w_o\Phi_d + Y_d(2,2)w_o\Phi_f + Y_d(2,3)w_o\Phi_{kd} \quad (2.16)$$

From equation 2.13 Φ_d is expressed as:

$$\Phi_d = [i_d - Y_d(1,2)w_o\Phi_f - Y_d(1,3)w_o\Phi_{kd}\ ]/[Y_d(1,1)w_o] \quad (2.17)$$

Similarly, equation (2.14) gives the relationship of Φ_q interms of Φ_{kq} and i_q,

$$\Phi_q = [i_q - Y_q(1,2)w_o\Phi_{kq}]/[Y_q(1,1)w_o] \quad (2.18)$$

Finally these new values of Φ_d, Φ_q and the current value of i_d and i_q are used in obtaining the voltages u_d and u_q as below :

$$u_d = w_o\Phi_q + R_a i_d \quad (2.19)$$

$$u_q = -w_o\Phi_d + R_a i_q \quad (2.20)$$

where $p\Phi_d$ and $p\Phi_q$ are neglected.

2.3 Ideal rectification process

In the brushless excitation system, the most important component is the rectifier unit. Therefore, representation of rectifier

unit plays an important part when modelling the brushless excitation system. A schematic diagram of the rectifier unit is shown in figure 2.2. The unit consists of six phase double way circuit. In analysing the above mentioned rectifier unit, two major assumptions are made for ideal condition. First, the ac power source is assumed to have zero reactance and secondly, the rectifier cells are considered to be perfect, in otherwords, they exhibit zero forward voltage drop.

The principle underlying behind the operation of the rectifier unit is governed by the relative magnitude of the phase voltages and also by the nature of load connected to its end. At a given instant, a particular diode conducts when its anode is connected to the phase of the highest positive voltage at that instant. Switching of current from one diode to another, commonly known as commutation, occurs when two phase voltage become equal and in the idealised system it occurs instantaneously. Figure 2.3 shows the effect of commutation on the rectifier voltages.

Considering rectifier A, figure 2.3 shows that, it starts conduction at $\pi/6$ i.e, 30^{o} and continues upto $5\pi/6$ i.e, 150^{o} whilst rectifier B then starts conduction instantaneously and continues upto 270^{o} which refers to the fact that each rectifier remains in conduction for 120^{o} of a cycle. Similar phenomena occurs for the lower bank of rectifiers D, E and F.

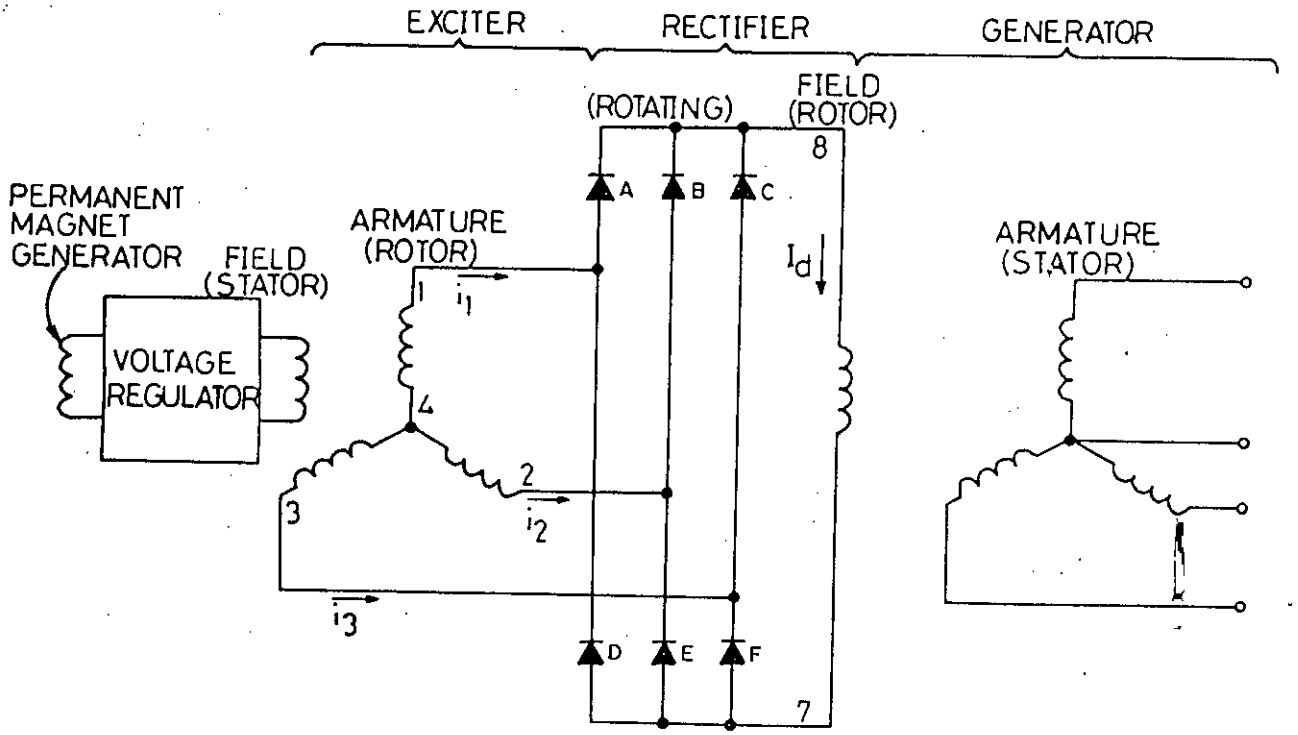

Fig. 2.2 A schematic diagram of brushless excitation system

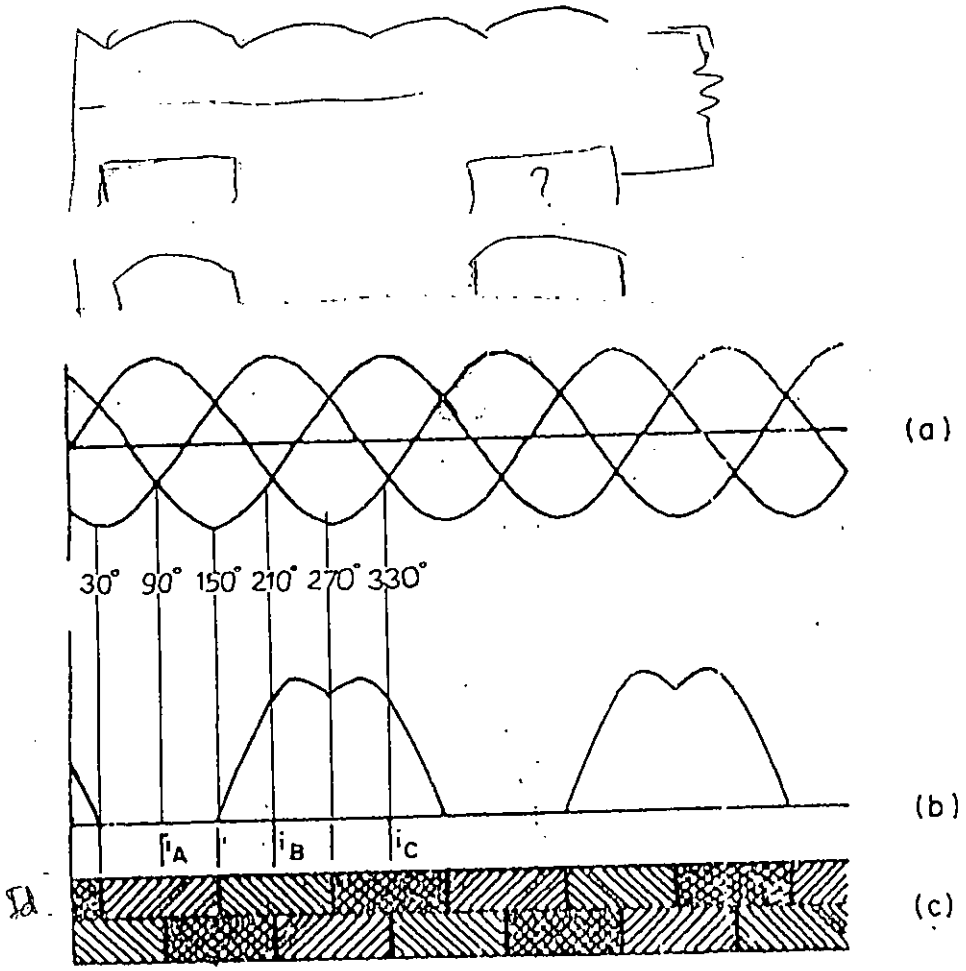

Fig 2.3 Idealised wave shapes for circuit of fig. 2.2

(a) Phase voltages

(b) Rectifier A voltage

(c) Line currents

The rectifier couple A and D contributes the current of phase 1, i_1 as shown in figure 2.3c. It exhibits that from $\theta = 30^o$ to $\theta = 150^o$, positive current of magnitude I_d constitute the current i_1 which flows through rectifier A. In the negative half cycle, the current passes through the rectifier D in the region of $\theta = 210^o$ to $\theta = 330^o$. In the intervals mentioned above, the current returns through other two phases, in turn. It is evident from the figure 2.3c that current switches from one phase to another phase at every 60 electrical degrees or six times per cycle.

2.4 Modes of operation in practical system.

The commutation process explained in the previous article is only valid for internal source impedance being zero. But in practice, there is always a predominantly inductive reactance inherent to the source. The phase to neutral reactance of the source opposes the transfer of current between rectifiers. The reactance is termed as the commutating reactance, X_c. This prevents the instantaneous transfer of current from one rectifier to another and so commutation requires a finite time which is defined by the commutating or overlap angle. It is a curious fact that the presence of commutating reactance forces the rectifier units to go through four distinct modes of operation as the load current is increased from zero to short circuit value by the variation of the effective load impedance and/or input voltage.

The wave shape of the first mode, called mode I, is discribed in figure 2.4. In the idealised case (see figure 2.3), the current in the phase 1 rises abruptly from 0 to I_D but in this case due to the presence of inductive source reactance, instantaneous transfer of currents is not possible. This is because of circulating current flowing from rectifier C to A as shown in figure 2.4d. In the figure 2.4, the current transfer from phase 3 to phase 1 is shown to extend from $\theta = 30^{o}$ to $\theta = 90^{o}$ and a similar transfer occurs in the negative phases. In the figure 2.4c, it is shown that in between $\theta = 90^{o}$ to $\theta = 150^{o}$, the rectifier A contributes the total positive current whilst negative phase currents are shared between rectifier E and F. But if the positive current transfer between rectifier A (phase 1) and rectifier B (phase 3) continues beyond $\theta = 90^{o}$, then it originates another operating mode.

The situation of the new mode is explained in figure 2.5. After completion of current transfer from phase 3 to phase 1 in the positive portion of the cycle, commutation starts between phase 2 and phase 3 in the negative portion when potential at point 2 and point 3 becomes equal. But if the transfer of positive current is extended beyond $\theta = 90^{o}$ the commutation in the negative portion is delayed. This is because, although the internal voltage of the phase 2 and phase 3 are equal at $\theta = 90^{o}$, but due to the flow of positive current, the potential at diode

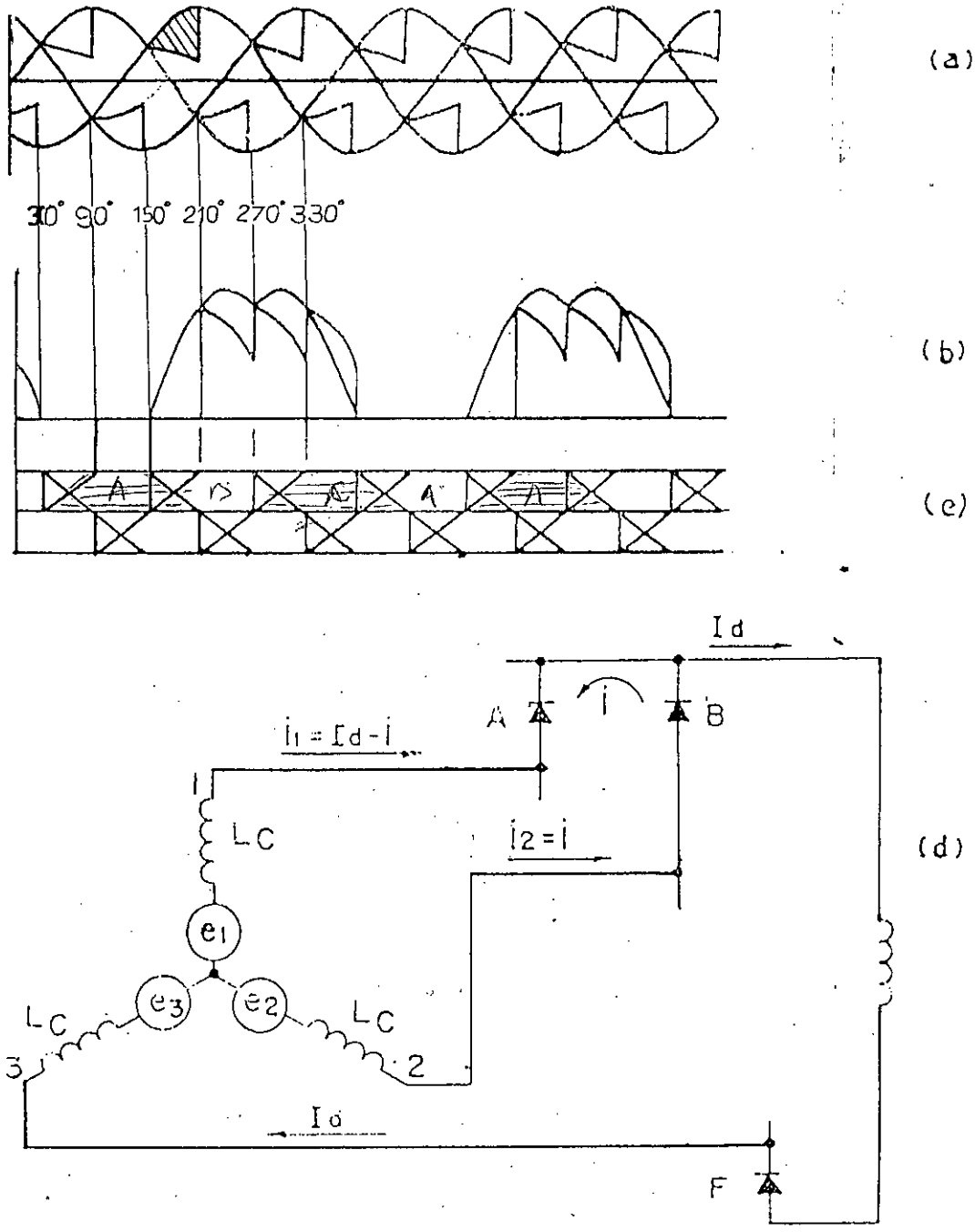

Fig. 2.4 Wave shapes and circuit diagram for mode

(a) Phase voltages

(b) Rectifier A voltage

(c) Line currents

(d) Circuit diagram

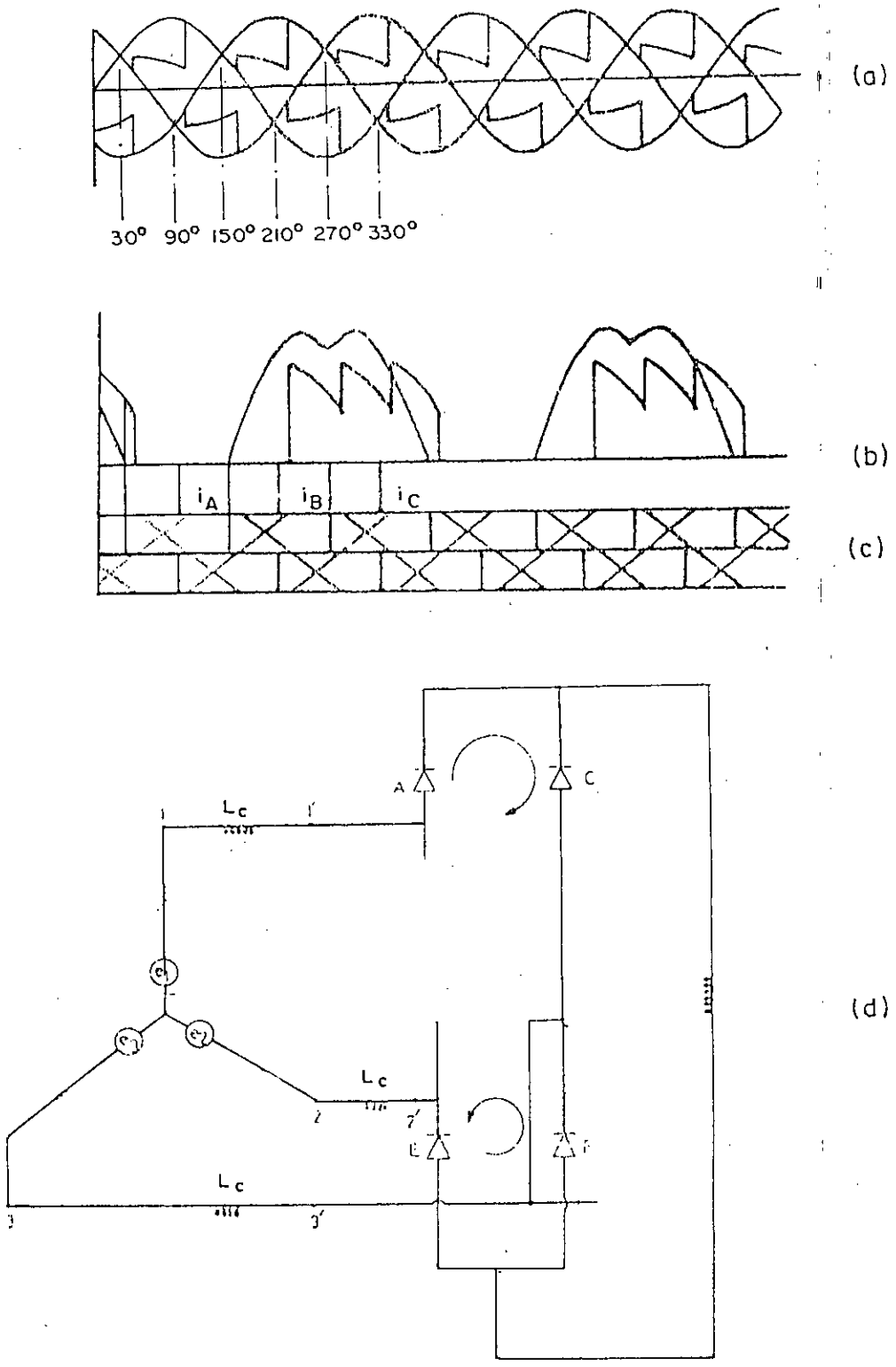

Fig. 2.5 Wave shapes and circuit diagram for mode II

(a) Phase voltages

(b) Rectifier A voltoge

(c) Line currents

(d) Circuit diagram

terminals, 2 and 3 are not equal. So, commutation between phase 2 and phase 3 starts after completion of the transfer of positive current from phase 3 to phase 1. In this mode, commutating angle being fixed at 60^{o}, every commutating interval is preceeded by a delay. This delay is qualified as delay angle (α). A waveshape corresponding to commutating angle (u) of 60^{o} and delay angle (α) of 15^{o} is shown in figure 2.5. The delay angle for this mode, called mode II, may extend upto 30^{o}.

If the delay angle becomes 30^{o}, a complete short circuit occurs between phases, because the voltages at the input of the rectifier A, B and F are then zero. So, commutation in the negative portion between rectifier E and F starts before the positive portion finishes commutation. This short circuit sustains until the transfer of positive current from phase 3 to phase 1 completes. Therefore, whilst the delay angle is fixed at 30^{o}, the commutation angle extends beyond 60^{o}. This new mode is called mode III and is explained by the wave shapes in Figure 2.6. In this mode, commutating angle may extend upto 120^{o}.

If positive current transfer from phase 3 to phase 1 is not complete at $u = 120^{o}$, then continuous short circuit sustains. This mode is termed as mode IV.

The commutation and delay angle for various mode of operation is summerised in the table 2.1.

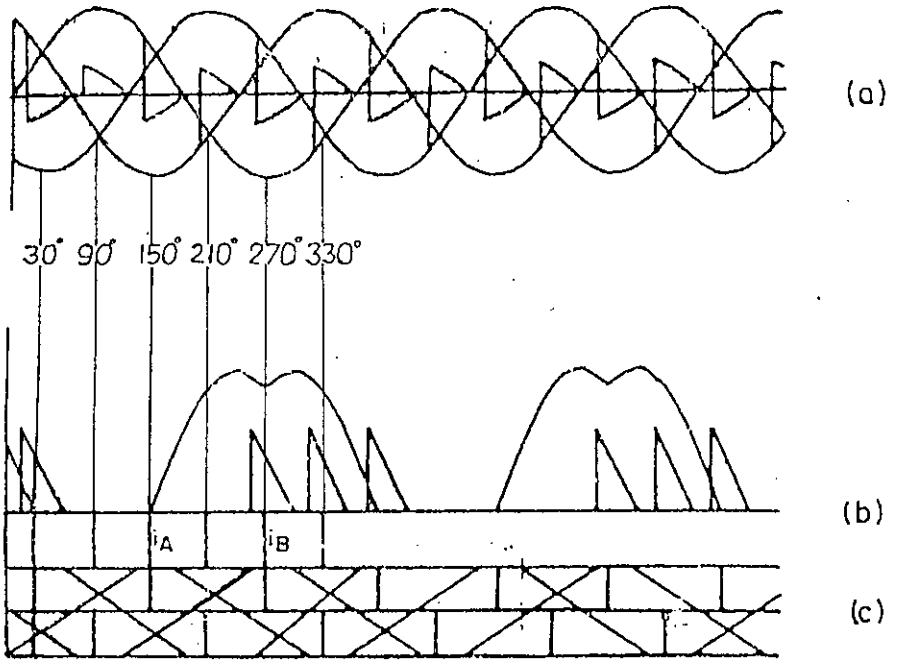

Fig. 2.6 Wave shapes for mode III

(a) Phase voltages

(b) Rectifier A voltage of fig. 2.2

(c) Line currents

Table 2.1

Commutation and delay angles for various mode

Mode	Commutating angle, u	Delay angle, α
I	$0 - 60^{o}$	0
II	60^{o}	$0 - 30^{o}$
III	$60^{o} - 120^{o}$	30^{o}
IV	120^{o}	30^{o}

2.5 Mathematical representation of different modes of operation

Assuming balanced sinusoidal phase voltages being fed to six phase perfect rectifier unit, the voltage e_1, e_2, e_3 are expressed as : (see figure 2.3a)

$$e_1 = V_E \text{Sin } wt \quad (2.21)$$

$$e_2 = V_E \text{Sin}(wt-120^o) \quad (2.22)$$

$$e_3 = V_E \text{Sin}(wt+120^o) \quad (2.23)$$

For simplicity the generator is expressed as a source of voltage behind commutating reactance, X_c . The diodes are expressed to be perfect and the resistance of the armature is neglected. The following analysis is based on the principle described in the previous article.

2.5.1 Analysis for mode I

Figure 2.4d represents the equivalent ckt for mode I. Applying KVL around the closed loop,

$$e_2 - e_1 = 2L_c[di/dt]$$

Replacing e_1 and e_2 by equations 2.21 and 2.22, becomes :

$$V_E [\text{Sin}(wt - 120^o) - \text{Sin } wt] = 2 L_c[di/dt] \quad (2.24)$$

Since in the figure 2.4d transfer of current from phase 1 to

phase 2 is shown to start at 150°, so the expression for instantaneous circulating current may be derived by integrating the equation 2.24.

$$i = V_E/(2L_c w_o) \int_{150^{\circ}}^{210^{\circ}} \sqrt{3}\ \mathrm{Sin}\ (wt - 150^{\circ})\ d(wt) \qquad (2.25)$$

which simplifies to

$$i = [\sqrt{3}V_E/2X_c](1 - \cos u) \qquad (2.26)$$

Since commutation ceases when $i = I_d$, so replacing i by I_d in equation 2.26,

$$\cos u = 1 - 2I_d X_c/[\sqrt{3}V_E] \qquad (2.27)$$

The voltage lost during one commutation interval is the value of the shaded area (see figure 2.4a) averaged over one cycle. The instantaneous value of this voltage is $[\ e_2 - (e_1+e_2)/2\ ]$ [i.e, $(e_2 - e_1)/2$]. Considering six commutation intervals in 360°, the average value of the total lost voltage is

$$\Delta E_d = 6 \times 1/2\pi \int_{150^{\circ}}^{210^{\circ}} V_E\ [\ \mathrm{Sin}\ (wt - 120^{\circ}) - \mathrm{Sin}\ wt\ ]\ d(wt)$$

$$\text{i.e, } \Delta E_d = 3\sqrt{6}\ (\ 1 - \mathrm{Cos}\ u)\ V_E\ /\ [\sqrt{2\pi}] \qquad (2.28)$$

Combining equation 2.27 and 2.28

$$E_d = 3 I_d X_c / \pi \qquad (2.29)$$

Now, by definition,

Rectifier output voltage at no load = Exciter rms phase voltage behind commutating reactance + Rectifier voltage drop due to commutation.

$$\text{i.e,} \quad E_{do} = \Delta E_d + E_d \qquad (2.30)$$

For sinusoidal phase voltage, the average value of no load rectifier output voltage is $3\sqrt{3}\ V_E / \pi$

$$\text{So,} \quad E_{do} = 3\sqrt{3}\ V_E / \pi$$

In otherwoards, from equation 2.30

$$3\sqrt{3}V_E / \pi = 3/\pi\ I_d X_c + E_d \qquad (2.31)$$

which gives

$$\boxed{E_d = 1.65\ [1 - 0.58\ I_d X_c / V_E]\ V_E} \qquad (2.32)$$

From equation 2.26 and 2.31, the expression for Cos u can be re-arranged as :

$$\boxed{\text{Cos } u = \frac{1 - 3/\pi\ (X_c I_d)/E_d}{1 + 3/\pi\ (X_c\ I_d)/E_d}} \qquad (2.33)$$

2.5.2 Analysis for mode II

For mode II, similar set of expressions as in mode I can be derived. In this mode, the commutation starts after a delay angle α and continues for interval of next 60° i.e, in this case commutation angle is fixed at 60° whilst delay angle α varies from 0 to 30°. Similarly as in mode I, the limit for the integrand of current ranges from $150^{\circ} + \alpha$ to $210^{\circ} + \alpha$,

$$i = \sqrt{3}[V_E/2X_c] \int_{150^{\circ}+\alpha}^{210^{\circ}+\alpha} \text{Sin}(wt - 150^{\circ})\, d(wt)$$

The solution gives :

$$I_d = [\sqrt{3}/2][V_E/X_c]\ \text{Sin}(\alpha + 30^{\circ}) \qquad (2.34)$$

$$\text{i.e,}\quad I_d X_c/V_E = \sqrt{3}/2\ \text{Sin}(\alpha + 30^{\circ}) \qquad (2.35)$$

The relationship between E_d and V_E for mode II can be established following the same procedure as explained for mode I. The relationship for this mode is :

$$E_d = [9/2\pi]\ \cos(\pi + 30^{\circ})\ V_E \qquad (2.36)$$

Replacing Cos $(\alpha + 30^{\circ})$ with the help of equation 2.35, the final expression for E_d becomes :

$$\boxed{E_d = 1.65\sqrt{[\ 0.75 - (I_d X_c/V_E)^2\ ]}\ V_E} \qquad (2.37)$$

Dividing equation 2.36 by 2.37, final expression for α can be derived as :

$$\alpha = \tan^{-1}\left[(9/(\sqrt{3}\pi)\ (I_d X_c/V_E)\right] - 30^{\circ} \qquad (2.38)$$

2.5.3 Analysis for mode III

In mode III, delay angle α being fixed at 30°, Commutation between two phases starts before the completion of transfer current between previous commutating phases. And so, a short circuit arises between the three phases. Referring to figure 2.6 commutation between phase 2 and 1 occurs in the interval between 180° (i.e., $150^{\circ} + 30^{\circ}$) to $180^{\circ} + u$. This interval can be divided into three distinct regions. First region 180° to $180^{\circ}+u- 60^{\circ}$, where a transfer of current between phase 3 and phase 1 occurs in addition to normal commutation. During $180^{\circ} + u- 60^{\circ}$ to 240° only normal commutation occurs. And, in the third region commutation between negative phases 2 and 3 occurs in addition to normal commutation as in the first case. Therefore all of the above three cases have the contribution to the total output current.

For normal commutation over total period :

$$2L_c\ [di/dt] = e_2 - e_1 \qquad \Big|_{180^{\circ}}^{180^{\circ}+u} \qquad (2.39)$$

which gives :

$$I_{d1}X_c/V_E = 1/2 \left[1 + 1/2 + \text{Sin}(u-30^\circ)-\text{Cos } u \right] \qquad (2.40)$$

The additional commutation current in the first interval is obtained from :

$$2L_c \left[di/dt\right] = e_3 - e_1 \Big|_{180^\circ}^{180^\circ+u-60^\circ} \qquad (2.41)$$

Similarly, the additional current in the third interval is described as :

$$2L_c \left[di/dt\right] = e_2 - e_3 \Big|_{180^\circ+u}^{240^\circ} \qquad (2.42)$$

Combining the solutions of equation 2.41 and 2.42 with equation 2.39 ($I_d = I_{d1} + I_{d2} + I_{d3}$), total current can be expressed as :

$$I_dX_c/V_E = 1/2 \left[1 + \text{Sin } (u-30^\circ)\right] \qquad (2.43)$$

For this mode, the relationship between E_d and V_E can be expressed as :

$$E_d = 9/2\pi \left[1 - \text{Sin } (u - 30^\circ)\right] V_E \qquad (2.44)$$

i.e,

$$\boxed{E_d = 1.65 \sqrt{3} \left[1 - I_dX_c /V_E \right] V_E} \qquad (2.45)$$

Combining equation 2.43 and 2.44

$$\text{Sin } (u - 30^{\circ}) = \frac{9/\pi \ (I_d X_c)/E_d - 1}{9/\pi \ (I_d X_c)/E_d + 1} \qquad (2.46)$$

2.5.4 Generalisation of different modes

For the ease of comparison the relationship between E_d and V_E for three modes and the expressions of commutation and delay angle for three modes are arranged in the table 2.2. From the table, it is evident that in order to distinguish the three modes of operation, one has to calculate either of the two different factors, commutation angle u or delay angle α. The deciding factor for mode I and III is commutation angle, u whereas delay angle, α is the deciding factor for mode II. But it has been discovered that the term $I_d X_c/V_E$ is common in the decisive factors for the three mode. This term may be used as the deciding factor of establishing a particular operating mode. Since 60° is the limiting final value of commutating angle, u for mode I, substituting the value in the expression of 'u', the value of $I_d X_c/V_E$ is obtained to be 0.433, similarly 60° is the limiting initial value of commutating angle for mode III. It gives the value of the factor $I_d X_c/V_E$ to be equal to 0.75. This term $I_d X_c/V_E$ is called as normalised current I_n . The value of this factor for different modes is tabulated in table 2.3.

Table 2.2

Expressions for different mode

	Relationship between E_d and V_E	Expression of u or α
Mode I	$E_d = 1.65[1-0.408\ I_dX_c/V_E]V_E$	$\alpha = 0$ $\cos u = \frac{1- 3/\pi(X_cI_d)/E_d}{1+3/\pi(X_cI_d)/E_d}$
Mode II	$E_d = 1.65[0.75-(I_dX_c/V_E)^2]V_E$	$u = 60^\circ$ $\alpha = \tan^{-1}(9/(\sqrt{3}\pi)(I_dX_c/V_E)$ -30°
Mode III	$E_d = 1.65\sqrt{3}\ [1 - I_dX_c/V_E]V_E$	$\alpha = 30^\circ$ $\sin(u-30^\circ) = \frac{9/\pi(I_dX_c)/E_d-1}{9/\pi(I_dX_c)/E_d+1}$

Table 2.3

Range of normalised current for different mode

Mode I	$0 < I_n < 0.433$
Mode II	$0.433 < I_n < 0.75$
Mode III	$0.75 < I_n < 1.0$
Mode IV	$I_n > 1.0$

It is relevant to mention that the ratio E_d and V_E, usually termed as loading factor, F_{ex} can also be related with the normalised current, I_n. The results after simplification are compiled in table 2.4. The curve showing the dependance of F_{ex} on I_n is known as regulation curve, which is shown in figure 2.7.

2.3.4 Resolution of phase currents in three modes

Examinations of the current waveshapes in figure 2.4 shows that the presence of commutating reactance produce two effects on the phase current pulses, (1) it displaces them in the lagging direction and (2) it distorts them by introducing slopes at the leading and trailing edges. Since it is difficult to derive expressions of the alternator phase currents for different modes, the rectified output is used to obtain, indirectly, the effective value of the alternator output currents. The alternator current is obtained in two steps. First, the real and reactive components of the phase currents are derived from the knowledge of rectified output current, the commutating and delay angle. components are derives. The relationship are [28] :

Real part :

$$A_1 = \sqrt{3}\, I_d/\pi \, [\, \text{Cos}\, \alpha \, + \text{Cos}\, (u + \alpha\,) \,] \qquad (2.47)$$

Table 2.4

Expressions for loading factors

Mode	Expression
Mode I	$F_{ex} = (1 - 0.58\ I_n)$
Mode II	$F_{ex} = \sqrt{(1 - I_n^2)}$
Mode III	$F_{ex} = 1.732\ (1 - I_n)$

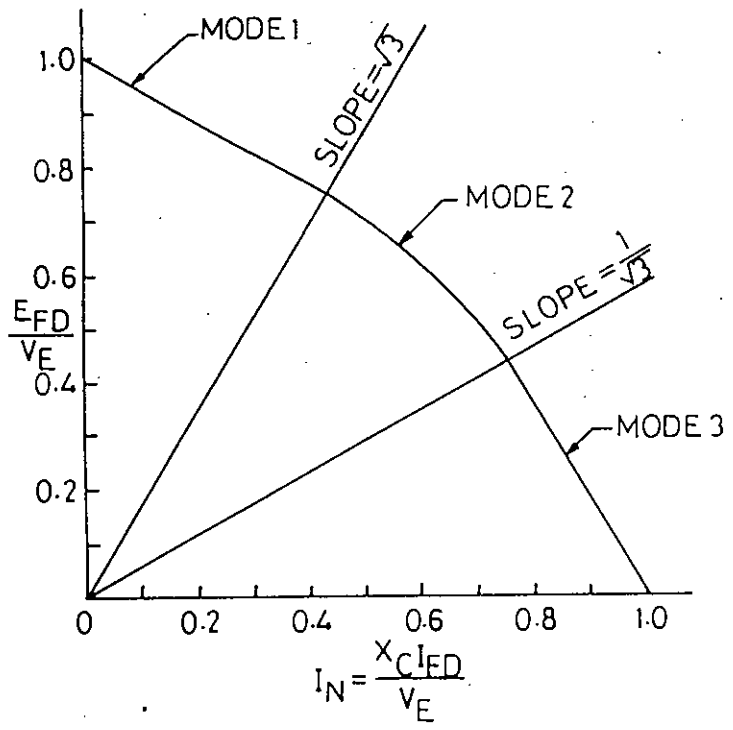

Fig. 2.7 Regulation curve for brushless excitation system.

Reactive part :

$$B_1 = 3/\pi\ I_d \frac{[\text{Sin } 2\ (\alpha + u) - \text{Sin}2\alpha - 2u]}{2\ (\ \text{Cos}\alpha - \text{Cos}(\alpha + u))} \qquad (2.48)$$

Once the real and reactive components are derived, the direct and quadrature axis components I_{de} and I_{qe} of the alternator current can easily be expressed with the help of the vector diagram as shown in figure 2.8 . The resulting equations relating A1 and B1 with I_{de} and I_{qe} are :

$$I_{de} = -\ (\ A1\ u_d + B1\ u_q\ )/V_E \qquad (2.49)$$

$$I_{qe} = -\ (\ A1\ u_q - B1\ u_d\ )/V_E \qquad (2.50)$$

The effect of delay angle, α has to be considered in resolving I_d and I_q in addition to that described by equations 2.49 and 2.50. This factor arises from the fact that the delay angle does not determine the load angle which is a function of load current. This shift of vector by the amount of delay angle is considered by the following equation :

$$I_d = I_{de} \text{ Cos } \alpha - I_{qe} \text{ Sin } \alpha \qquad (2.51)$$

$$I_q = I_{qe} \text{ Cos } \alpha + I_{de} \text{ Sin } \alpha \qquad (2.52)$$

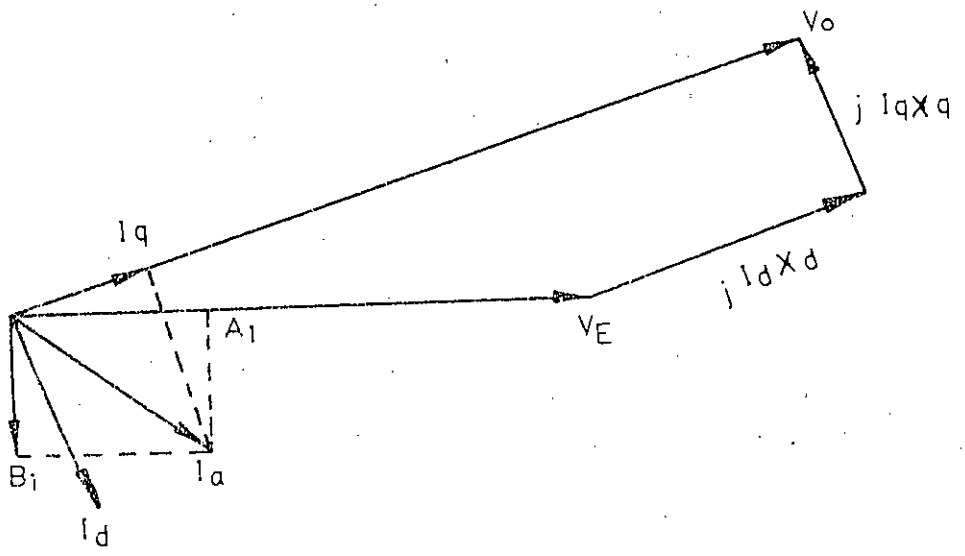

Fig. 2.8 Phasor diagram of an alternator.

Chapter 3

EXCITATION TO AN ALTERNATOR WITH NO LOAD

3.1 Program layout for the simulation:

The brushless excitation system with exciter rectifier and alternator as one unit is modelled on the basis of the following steps.

1. The field voltage corresponding to 1.0 pu open circuit terminal voltage is obtained by multiplying the corresponding field current with field resistance R_f. The field current is defined as $\sqrt{2}/X_{md}$ pu which is obtained from open circuit characteristics of the alternator [27].

2. The terminal voltage is determined from the resultant of direct and quadrature axis voltages. To calculate the direct and quadrature axis voltage, rate of change of flux is required. These values are achieved from equation 2.15. The equation requires elements of admittance matrix of the machine, which is obtained by inverting the impedance matrix. Again, the impedance matrix is composed of machine's equivalent circuit parameters.

3. To distinguish the different operating mode, normalised current, I_n is calculated from the knowledge of previous values of alternator field current, commutating reactance and terminal voltage . According to a particular mode, the corresponding loading factor, F_{ex} is established from the regulation curve is described. 4. The field voltage E_{fd} of the main alternator is

obtained by multiplying the terminal voltage of exciter alternator V_E and loading factor F_{ex}. Considering E_{fd} as the input to the main alternator, the equation of rate of change of fluxes for the main alternator is solved similarly as described in step 2. New fluxes of the alternator give the load and field current of the same.

5. Since the d.c. field current of the main alternator is a resultant effect of three phase currents of the exciter alternator, the d.c. current is first resolved into real and reactive parts and consequently into direct and quadrature axis components. The effect of delay angle is then included in the component currents. These components are used in calculating terminal voltage of the exciter in step 2.

6. The steps from 2 to 5 are repeated for next time steps and field currents and output voltage are stored. In the present study time step was chosen as 10 msec.

3.2 Data for the excitation system

To investigate the computer model developed for the brushless excitation system, test results [29] of a physical laboratory model was used. The physical model at university of manchester consists of a salient pole micro-machine supplying field of another cylindrical rotor micro machine through a 3-Ø diode

rectifier unit. The machines were of rating 3KVA, 220V, 1500 rpm. The machine parameters were obtained from 3-Ø short circuit test at the machine terminal. The equivalent circuit of the machine is represented as the form suggested by Canay [22]. The circuit parameters for the exciter-alternator and that of main alternator are given in figures 2.1 and 3.1 respectively.

3.3 Response to an step voltage at exciter input

In order to eliminate the complexity of the total system and to check the validity of the equation derived for various modes of operation, it was decided to simulate the response of an exciter keeping main alternator at no load. Considering initially relaxed excitation system, a sudden exciter voltage was applied at the field of the exciter-alternator. The output voltage at the rectifier end was impressed across a passive R-L circuit representing the field of the main alternator. The simulation was carried out in two different ways. One was based on the present analysis and the other was on the basis of IEEE model [20].

3.3.1 Simulation using present analysis

The machine representation was based on park's two axis theory. The differential equations for the machine and the field current were solved by Runge-Kutta routine. The mode of operation at each

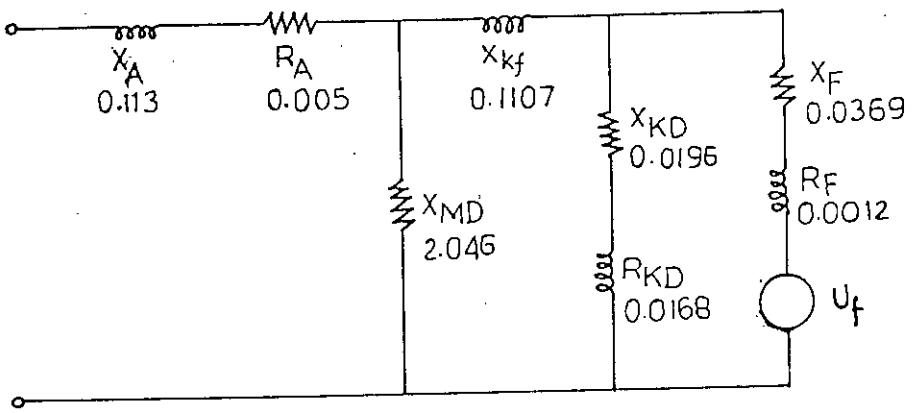

(a) Direct axis

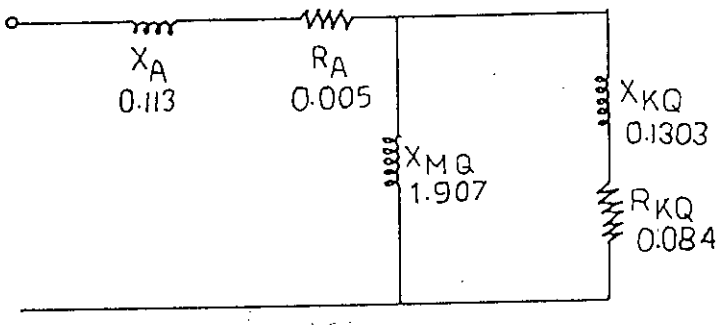

(b) Quadrature axis

Fig. 3.1 : Equivalent circuit of d q axis model of the main alternator.

instant of solution was decided from the equation described in chapter 2. The d- q components of load current were derived from the d.c. field current at the rectifier end using the knowledge of particular mode of operation. This components were considered in determining the exciter-alternator terminal voltage.

The response of an unloaded alternator following an step voltage at the exciter input is shown in figure 3.2 along with test result. The field current of the exciter increases more rapidly than the field current of the alternator and the maximum value of the field current of the exciter occurs earlier than the field current of the alternator. The facts are consistent with respect to relative magnitude of parameters in the two field circuits. The effective time constant of the exciter field circuit is lower than that of the alternator field circuit.

It is observed that the rectifier operates in mode I until the current approaches their peak value. The relative magnitude of the two current during the decreasing portion is such that the mode changes from mode I to mode III via a small interval of mode II. Before reaching the final value, the currents experienced a slow oscillation. The final mode of operation was found to be in mode II. This curve also exhibits a comparison of peak values of the currents. In per unit sense, the peak value of the exciter alternator field current is seen to be greater than that

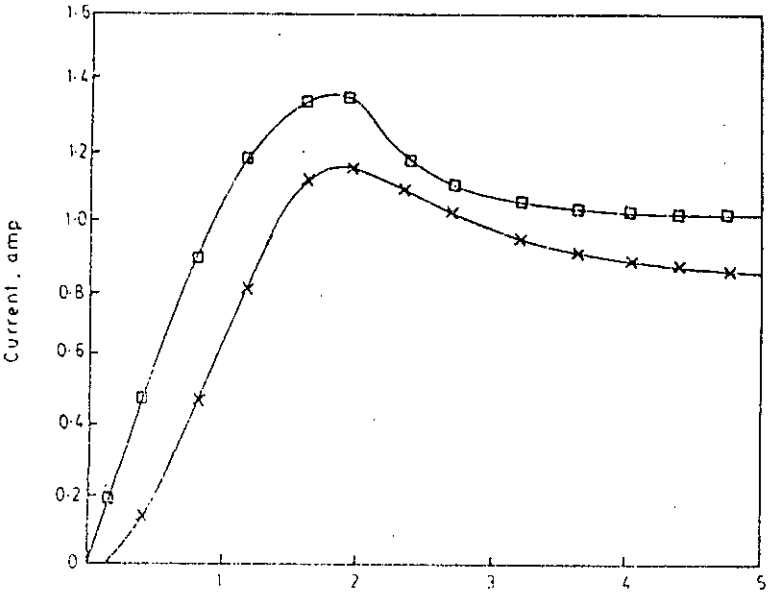

(a)

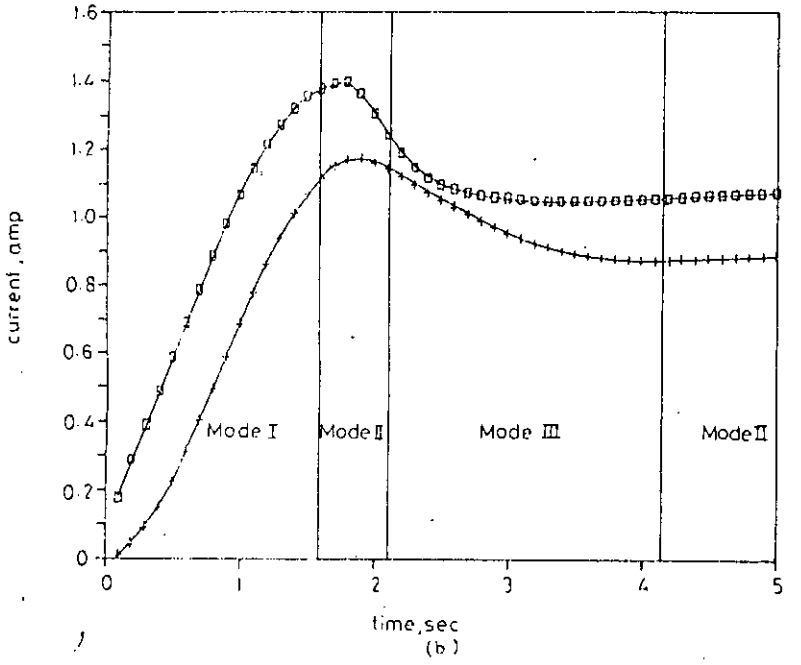

(b)

Fig. 3.2 Response of field currents due to sudden application of exciter field voltage of an alternator at no load

R_{fd} = 0.75 PU L_{fd} = 1.125 PU

O -- O exciter

+ —— + alternator

a. test

b. simulated

of main alternator. Their relative magnitudes are important in designing the excitation system.

3.3.2 Simulation using IEEE Model

With the advent of new excitation system, IEEE excitation sub-committee reviewed the existing models in 1981 [20]. A block diagram of modelling brushless excitation system is presented in Reference [20]. The diagram is reproduced in figure 3.3. This model consists of a exciter with non-controlled rectifiers to produce the direct current needed for main alternator field. The principal input to this model is the step unit voltage u_f. The exciter alternator is represented by a simple time constant. The terminal voltage of this alternator is used to determine the normalised current, I_n (see section 2.3). Normalised current is also related to the commutating reactance X_c and load current I_{fd}. The different modes have different loading factor F_{ex} which is the function of normalised current, I_n. By multiplying the term F_{ex} and rectifier terminal voltage V_E gives the exciter output voltage E_{fd}. This voltage is applied to the field of the main alternator and field current I_{fg} is obtained. This I_{fg} is fedback to the exciter input which affects the exciter output voltage. A constant of K_d is used as feedback factor.

A program was developed on the basis of the block diagram shown in figure 3.3. The response of exciter step voltage was simulated

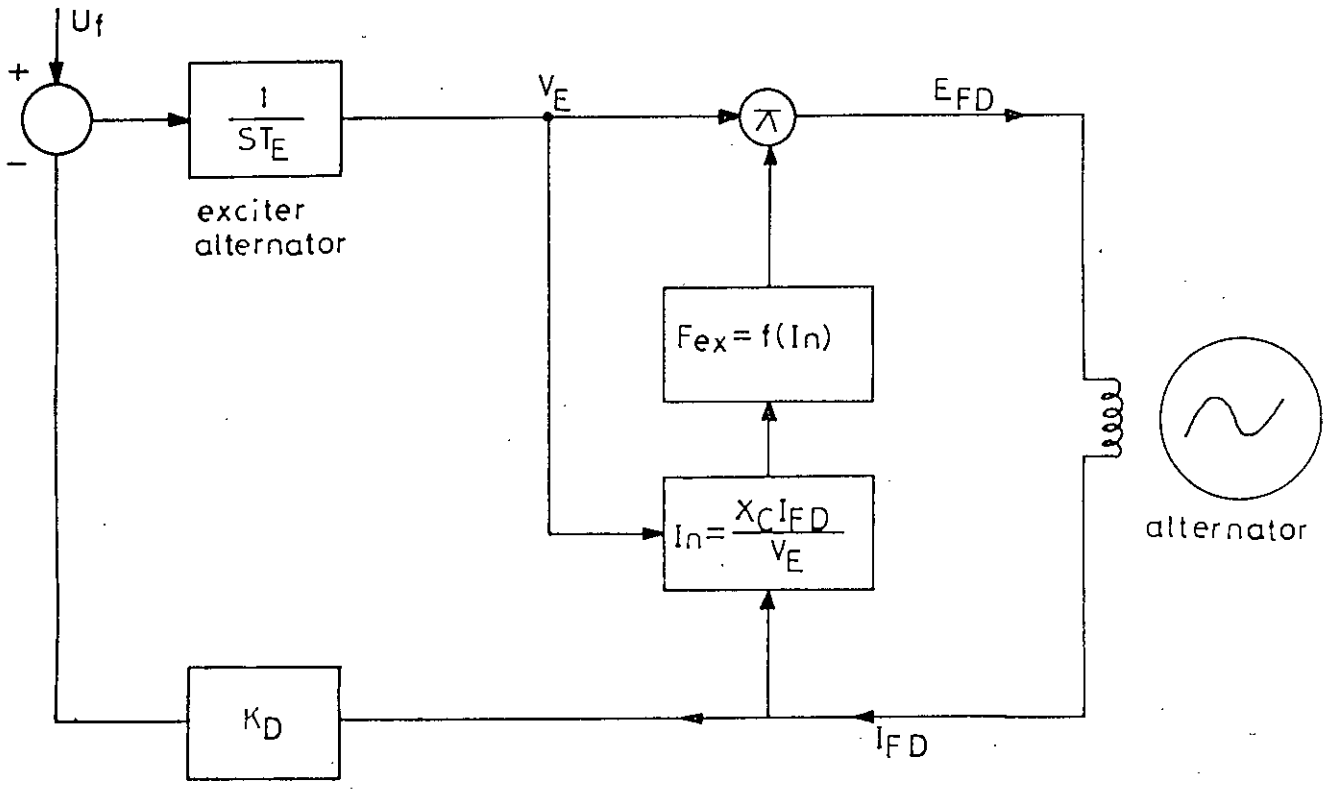

Fig 3.3 : IEEE model of the brushless excitation system.

and shown in figure 3.4. A poor agreement to the IEEE model's response with the test result of figure 3.2 was observed. The shortcomings of IEEE model was pointed out as below :

(a) In the IEEE model, the exciter alternator is represented by a single time constant. Representing machine by a single time constant is only applicable for a machine under no load. When a load is connected, flux will be developed in both the d- and q-axis. Effect of distribution of flux in the two axis becomes important specially when machine is a salient pole one. Since, in the brushless excitation system, salient pole type machine is used as the exciter alternator so the exact result can only be achieved if single time constant exciter-alternator model is replaced by two axis model. In this view, d-q axis model for the machine has been incorporated in the present investigation.

(b) The effect of load current in the IEEE was incorporated from a phasor diagram corresponding to a particular instant. The phasor diagram provides the voltage at no load and that under load condition. The ratio between there two quantities was being considered as the feedback factor K_D. Since the phasor diagram was based on direct axis parameter only the constant K_D does not provide the correct measure of feedback factor.

(c) The effect of delay angle on the resolution of load current has not been taken into account in the IEEE model. This

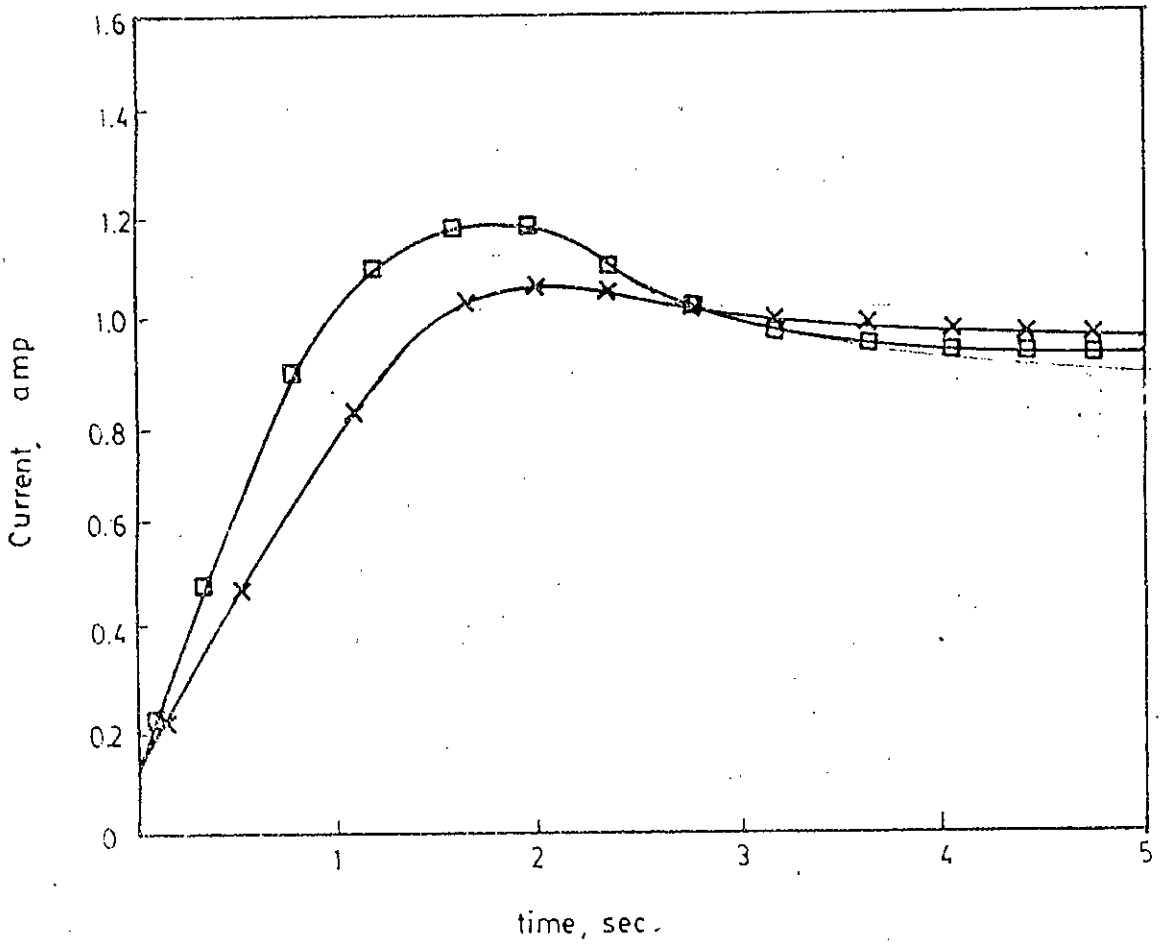

Fig. 3.4 Response of IEEE model

□ Exciter field current

× Alternator field current

consideration was found to be essential in obtaining accurate response of the exciter.

3.4 Effect of field resistance

It is obvious fact that field and damper resistance varies from machine to machine according to their size. For a large machine, the resistances are small whilst they are high for machines of its smaller counterpart. The design engineer has to know the effect of various field resistance on transient performance of exciter system. Hence in the present study it was decided to run the program for different values of field resistance. The response of the exciter field current for various field resistances are shown in figure 3.5. When the resistance of the exciter field was increased by ten times of the normal value, then the peak arises earlier whereas it appears later when the resistance of exciter field was decreased by ten times. This was because, the time constant of the machine is inversely proportional to the field resistance. On the otherhand, the increase or decrease of field resistance have direct influence on the peak value of the currents.

3.5 Effect of the damper resistance.

The effect of damper resistance of the exciter alternator is also

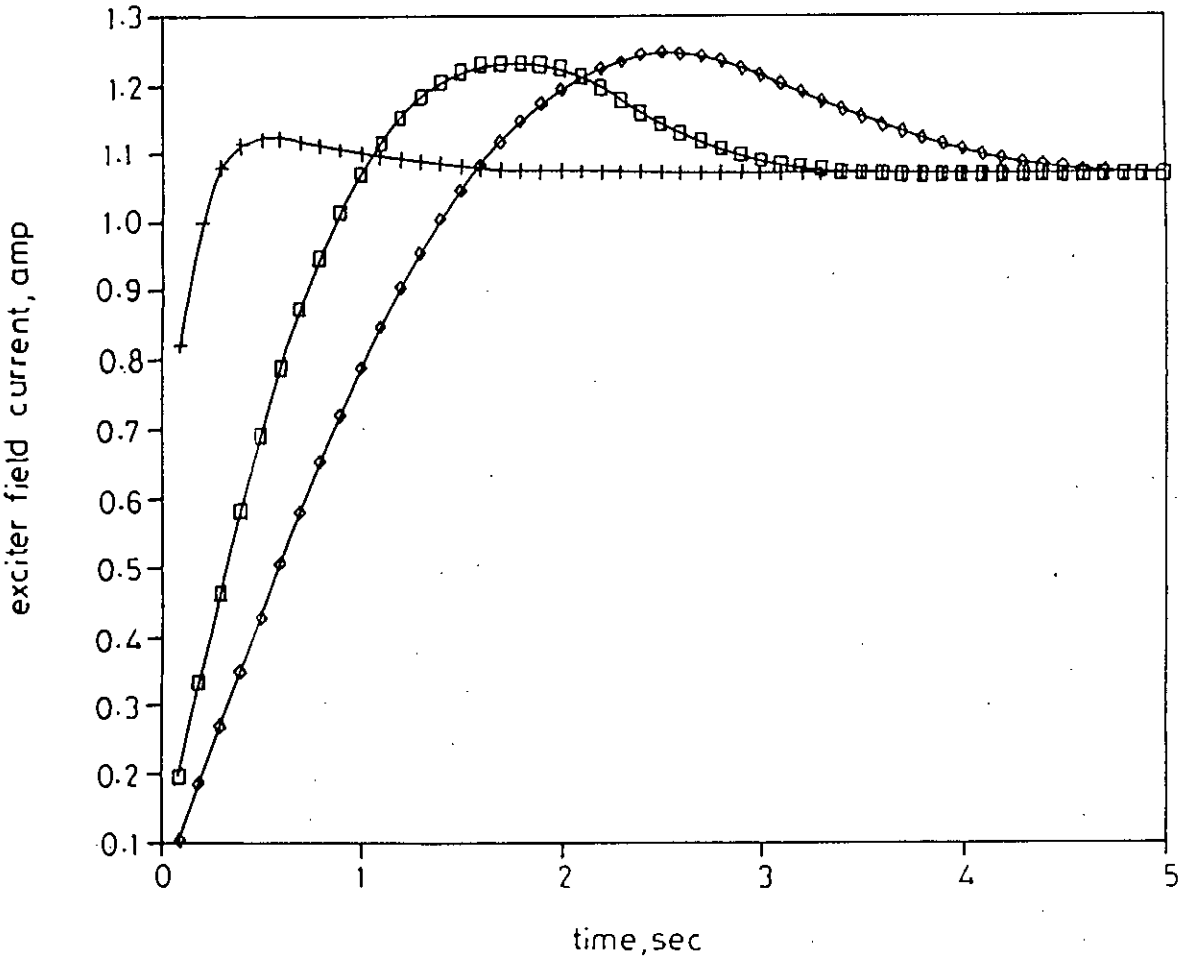

Fig. 3.5 : Effect of exciter field resistance on its field current.

□ — □ $R_f = R_{f1}$

◇ — ◇ $R_f = R_{f1}/10$

\+ — + $R_f = R_{f1} \times 10$

(R_{f1} = 0.00651 PU)

an important investigation to be made. This is important, because the damper resistance may be of different values according to the rotor type. Depending on type of material and type of lamination provided in the rotor, the damper resistance varies. This is true for both d- and q- axis damper resistances.

The figure 3.6 shows the effect of varying direct axis damper resistance of the exciter on its field current whilst the figure 3.7 shows the effect of varying quadrature axis damper resistance.

The effect of increasing resistance could not be exhibited clearly, because the increase in d-axis damper resistance beyond twice of its normal value caused numerical instability in the computation. On the otherhand, the decrease in d-axis damper resistance affects the output response as expected. It agreed with the fact that as d-axis damper resistance is decreased, the flux in the damper takes more time to penetrate. Hence the current takes longer to reach the peak value.

The effect of changes in q-axis damper resistance was negligible as seen in figure 3.7. This was because, the quadrature axis flux should have less control over field current which contributes the flux in the direct axis only. This once again verifies the fact that the representation of the quadrature axis with one damper circuit is adequate in modelling alternator [26].

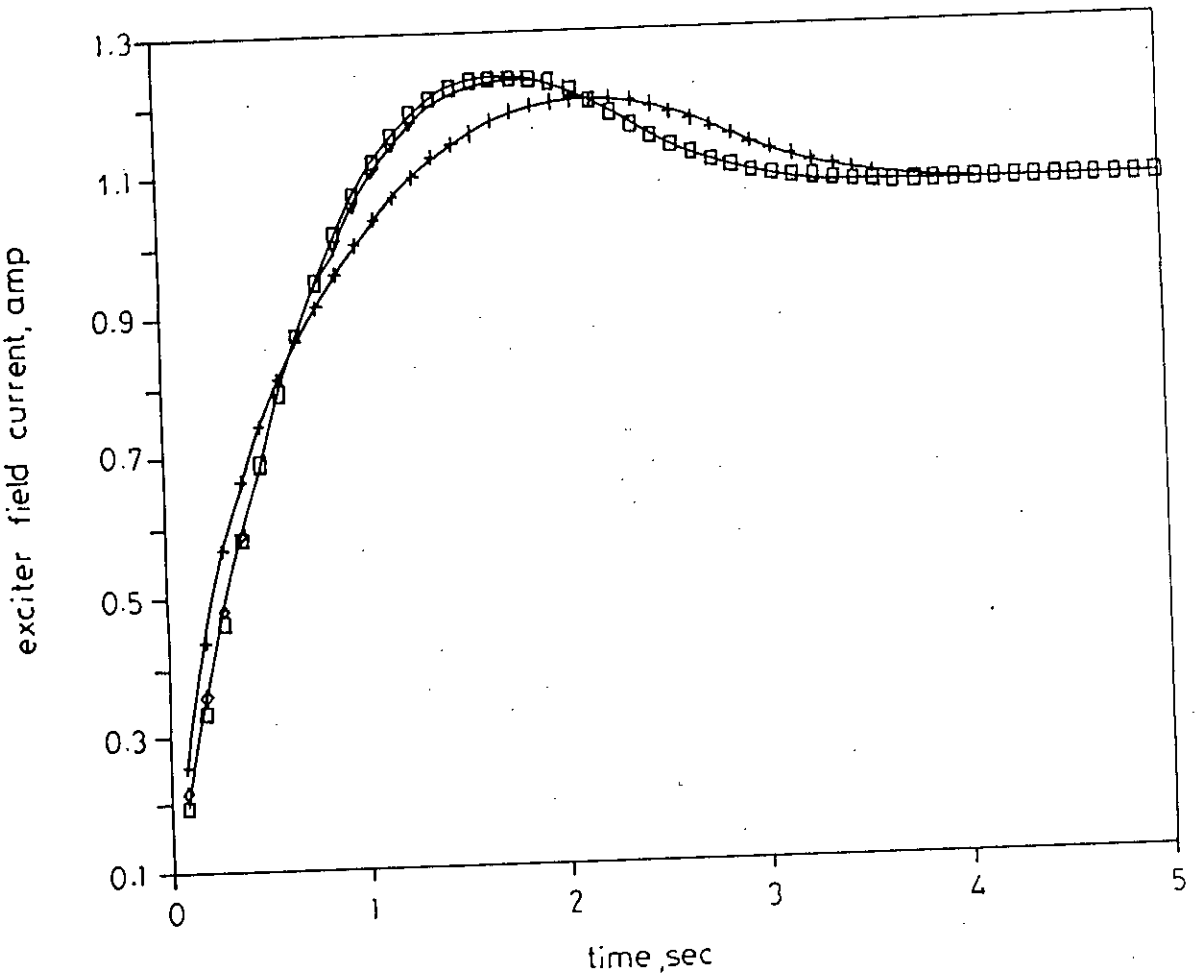

Fig. 3.6 : Effect of d-axis damper resistance of the exciter on its field current.

□ — □ $R_{kd} = R_{kd1}$

\+ — + $R_{kd} = R_{kd1/10}$

◇ — ◇ $R_{kd} = R_{kd1} \times 2$

($R_{kd1} = 0.06905$ PU)

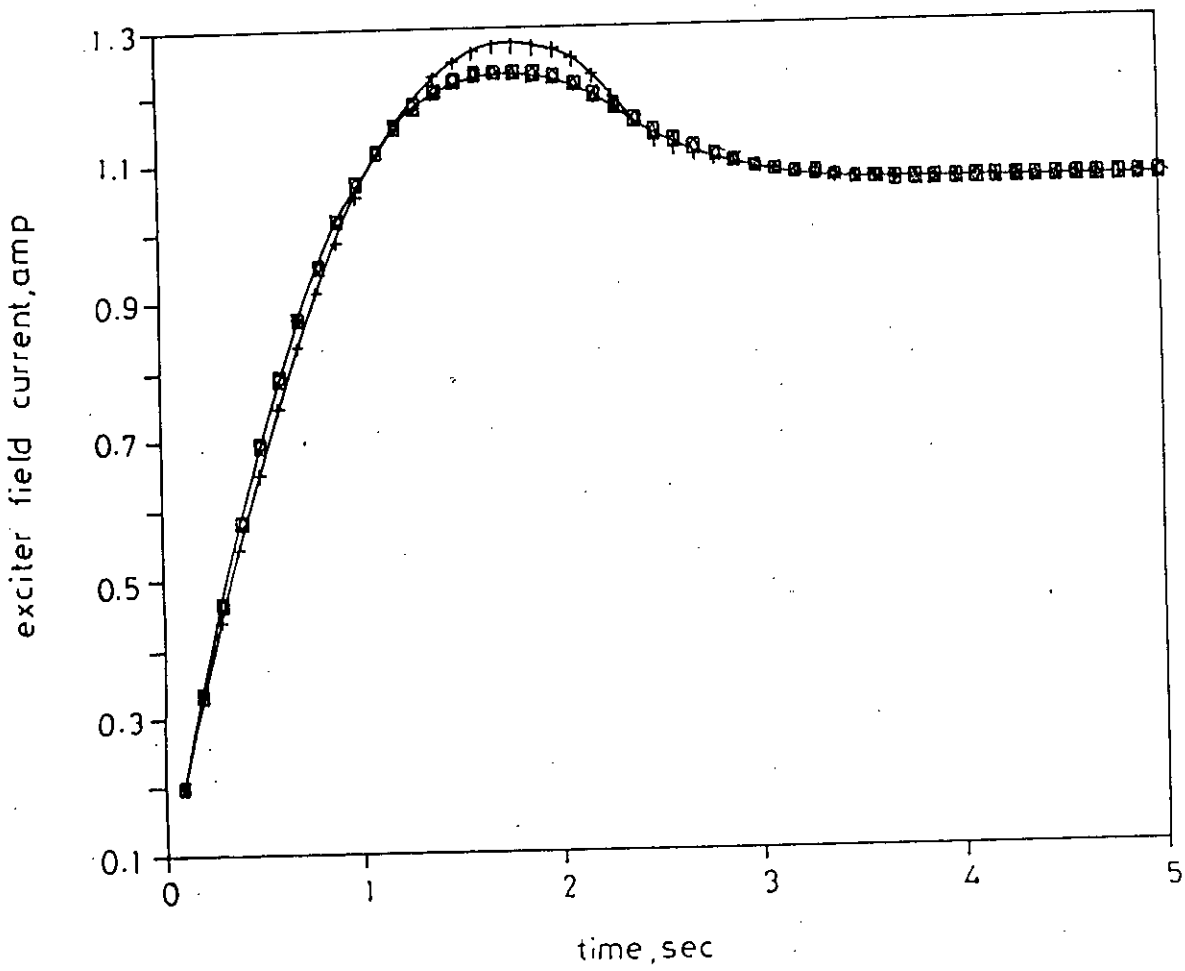

Fig. 3.7 : Effect of q-axis damper resistance of the exciter on its field current.

□ — □ $R_{kq} = R_{kq1}$

\+ — + $R_{kq} = R_{kq1}/10$

◇ — ◇ $R_{kq} = R_{kq1} \times 2.5$

($R_{kq1} = 0.55$ PU)

Chapter 4

EXCITATION TO AN ALTERNATOR WITH LOAD

4.1 Introduction

After varifying the exciter-rectifier model, a practical system with brushless excitation system was simulated. In this case, the main alternator was considered to be loaded and the effect of field excitation on the alternator load and field current was studied. Besides this, the effects of short circuit at the main alternator end, load switching and change in power factor of the load on the brushless excitation system were also investigated. In addition to transient study, steady state performance of the brushless excitation system has also been studied.

4.2 Modelling alternator at the exciter end

The main alternator, the field of which is supplied from the rectifier output, was modelled in the similar process as described in section 2.2. The alternator is represented in the conventional d-q axis and parameters were obtained from the Canay's equivalent circuit. The value of the parameters are given in figure 3.1. As in the previous case, the representation did not include the rate of change of direct and quadrature axis fluxes and hence a time step of 0.01 sec was maintained. The voltage at the field of the alternator was obtained from the rectifier output voltage. The rate of change of field and damper fluxes were calculated at each time step. The updated value of

these fluxes were used to calculate d-q axis load current and field current of the alternator. Since the field current of the main alternator constitutes the load of the rectifier unit, the current was fedback to the exciter alternator following the procedure described in section 2.2.

4.3 Response of a loaded alternator

The effect of step voltage at field end of the exciter alternator was described in the previous chapter. The response was only valid for static load at the rectifier end. Since it is of practical importance to observe the similar effect when the rectifier load is of dynamic kind , i.e. a rotating alternator with load at its end. The model was modified to incorporate the dynamic load of the exciter. The main alternator was considered to be supplying passive loads of constant values. First, the load was assumed to be connected before a step voltage at the field of the exciter alternator was suddenly applied. The curve representing the response of the field current of exciter alternator under loaded condition is shown in figure 4.1b. A similar curve for no load condition is redrawn on the figure 4.1a. Curves for field current of main alternator are demonstrated in figure 4.1b.

It can be observed from the figure 4.1 that currents in the

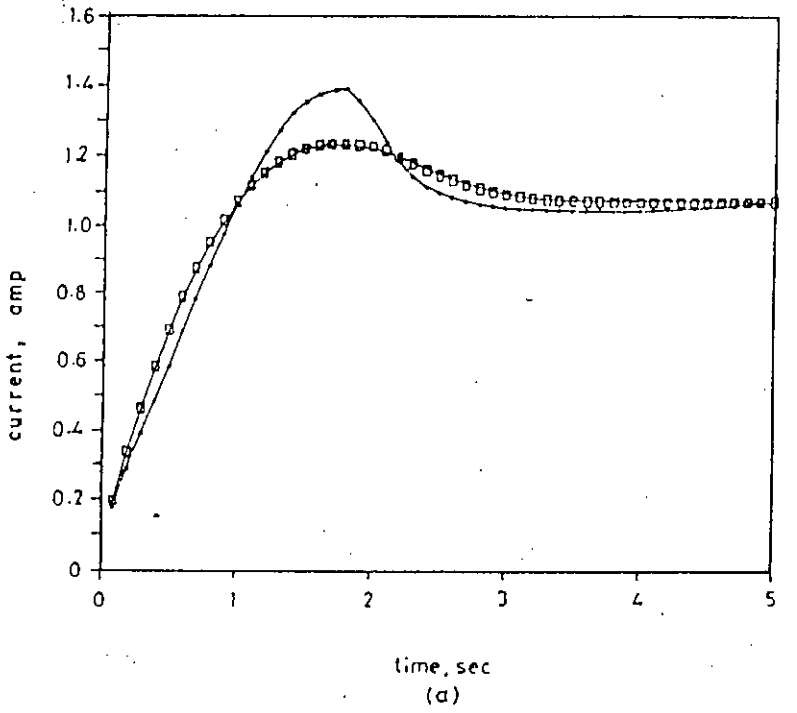

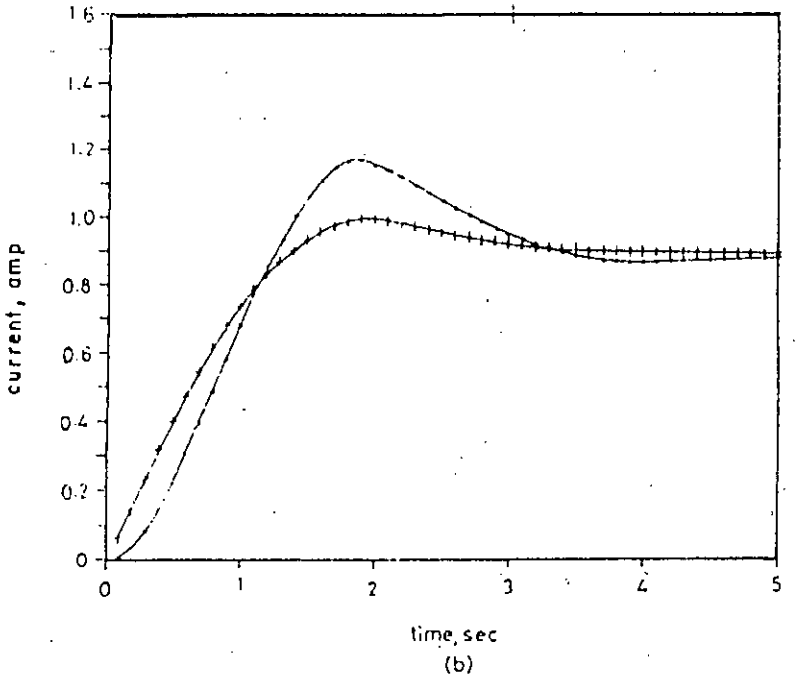

Fig. 4.1 Response of the field current.

+ + No load condition

• • Loaded condition

(a) Exciter field current

(b) Alternator field current

machine with load connected have lower peak value and they occur a bit earlier than currents in machine with preload. Due to the addition of load, the transient fluxes take more time to rise and hence the currents rise to a lower value at the time of peak. The decay of currents after the occurance of peak are also seen to follow a slower rate due to longer time constants of the system.

It may be concluded that due to lower peak of currents the switching of field is safer in case of an alternator when connected to a load.

4.4 Effect of load switching

It is common practice in power system to increase or decrease loads time to time. Therefore, it becomes apparent for the present study to investigate the effect of load switching in the brushless excitation system. For this purpose, the model developed was modified to facilitate the investigation. The load impedance was lumped together with armature leakage reactance and resistance. The modified machine was considered to have a short circuit at its end. The transient condition was simulated by keeping the exciter field voltage constant, whilst changing the value of load resistance and/or load inductance of the re-arranged alternator model. The load switching was studied for alternator with preload. The pre-loaded situations were obtained

by running the program with parameters valid for preload condition and when the final value was reached, the load parameters was changed corresponding to the new situation. The effect of changing a load of unity power factor has been simulated for this type of study. The result is shown figure 4.2. and figure 4.3. Figure 4.2 demonstrates the effect for decreasing load for preloaded value whereas the effect of increasing load is depicted in figure 4.3.

In each figure, it has been noticed that a sudden step of current change occurs just after switching. The change in the case of decreasing load was approximately three times of the final change whereas the step change of current was approximately six times of the final change in the case of increasing load. This is due to the fact that when load was increased, the impedance connected the machine decreased which in turn offered stronger shock to the load change. The shock was less in the case of decreasing load because of the opposite reasonning.

It is therefore important to conclude that the step load change in the increasing direction is more severe than that in the decreasing case.

4.5 Effect of short circuit at the main alternator terminal

Short circuit study is an important investigation in power

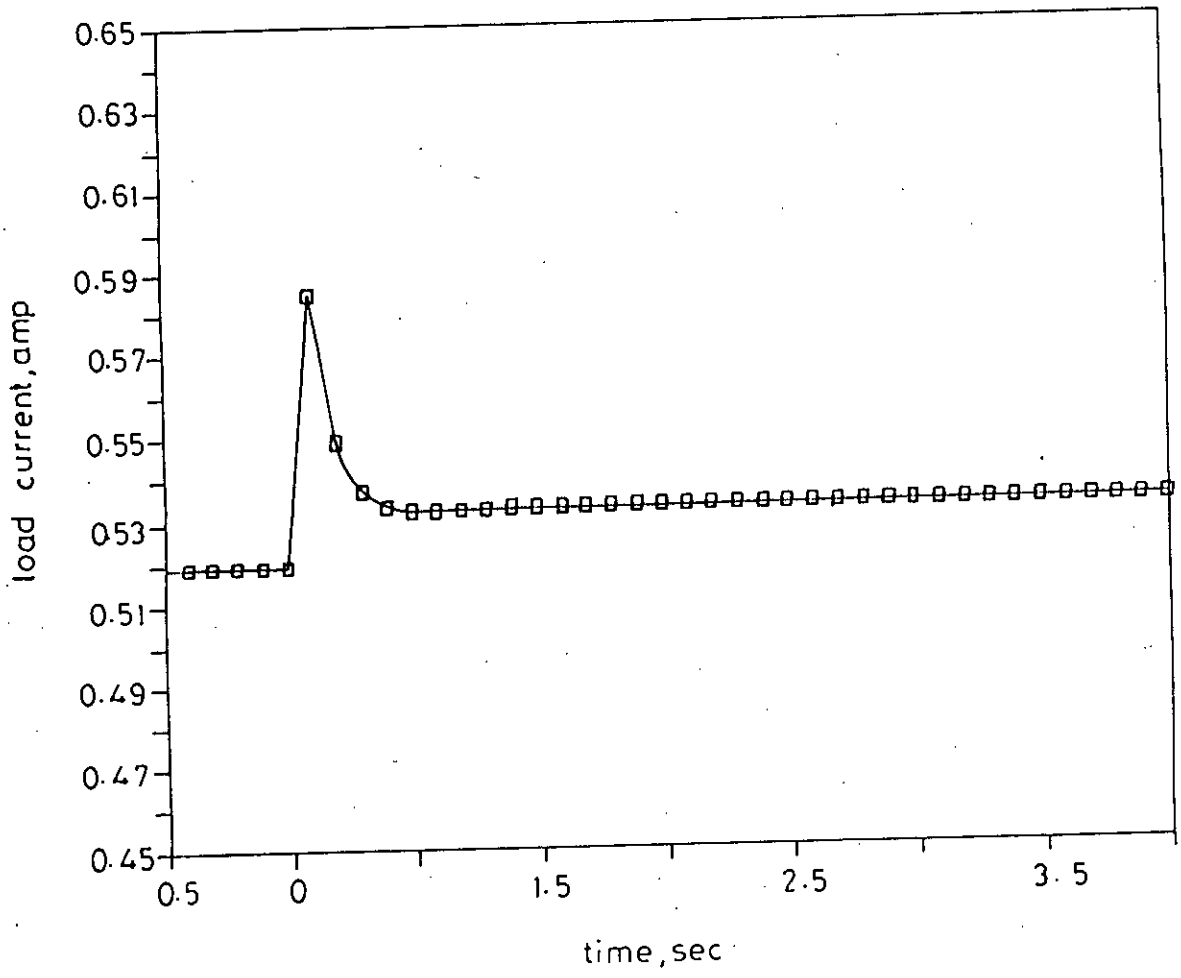

Fig. 4.2 : Effect of sudden decrease in load resistance on load current.

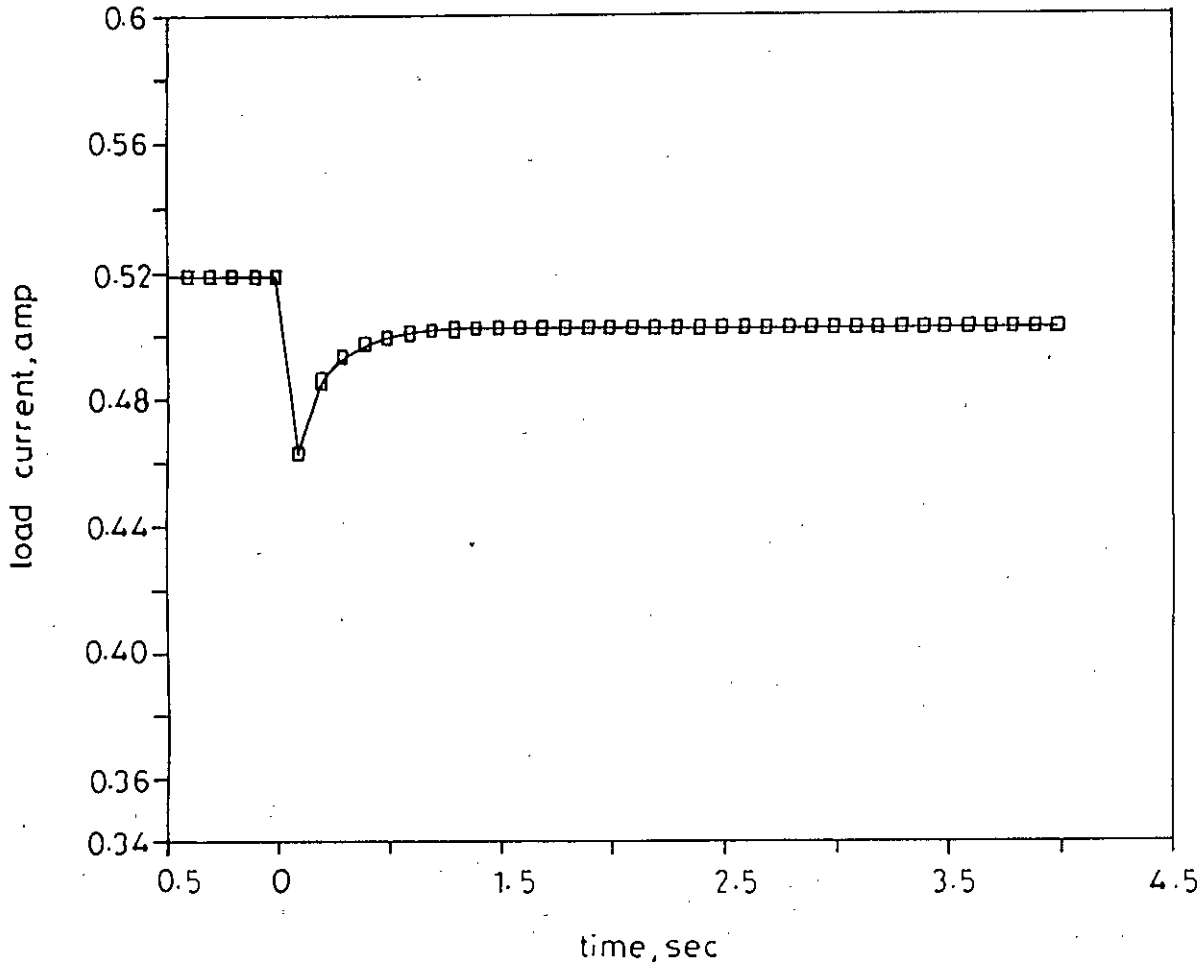

Fig. 4.3 : Effect of sudden inerease in load resistance on load current.

system, because of its frequent occurance in practice. Therefore, it was decided to use the brushless excitation model to investigate effect of short circuit on the excitation system. The short circuit situation was simulated by setting external impedance to zero. The short circuit at the machine terminal was initiated with machine both at no load and preloaded condition. The results are presented in figure 4.4.

In the preloaded case, the preload current was of unity power factor, so the flux was lying in between d- and q-axis which means the d-axis component is less than the excitation flux. Since the direct axis flux determines the post fault short circuit current hence the currents for the preloaded machine were less than those for the machine at no load.

4.6 Steady state response

4.6.1 Simulation procedure

It has been mentioned earlier that for designing an exciter alternator transient behavior of the system must have to be known. The behavior includes the response at any kind of switching or fault conditions. Besides the transient study, the steady state characteristics of an excitation system are equally important for normal operation of the system. The necessary field current under a particular steady state load condition needs to

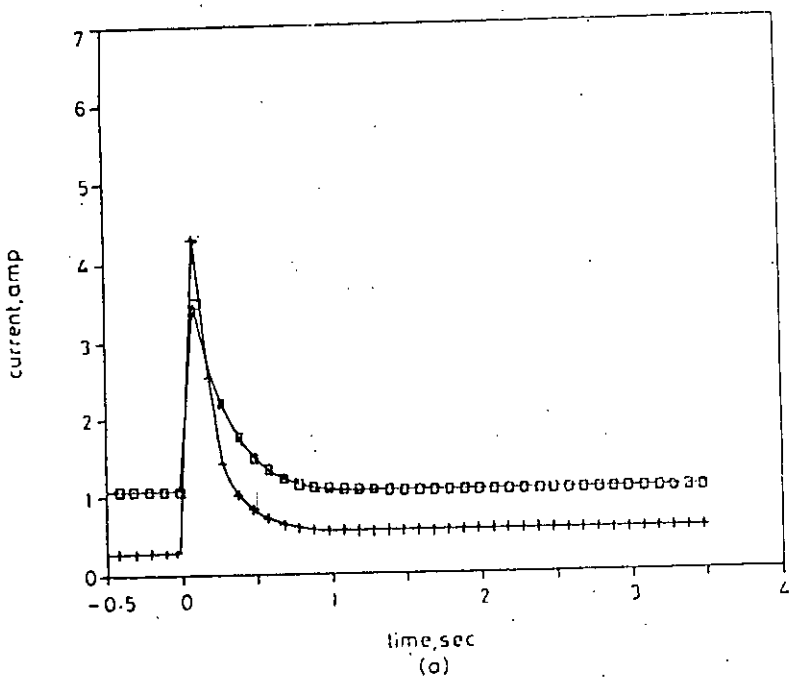

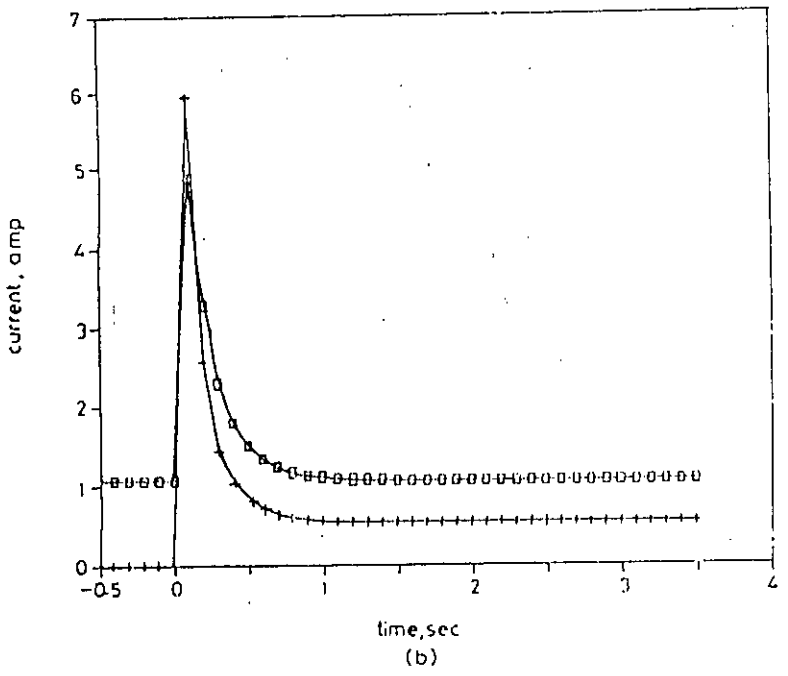

Fig. 4. 4 : Simulation of alternator currents due to application of sudden short circuit at the load end.

+ — + load current

□ — □ field current of the exciter.

(a) From pre-loaded to short circuit condition.

(b) From open circuit to short circuit condition.

be known in deciding the voltage regulator parameters. In this study, load current versus field current for a particular terminal voltage and at fixed power factor was obtained. The calculation was performed indirectly.

The transient program was used to achieve the final value at steady state. The operating mode at a particular load condition was found to be difficult to calculate directly. The factors relating the operating mode are so dependent that determination of one factor depends on the known value of the other. Therefore, a long procedure had to follow to calculate steady state performance. The procedure was to use the same transient model with reduced computation time. The computation time was reduced by increasing the exciter alternator field resistance and thereby decreasing time to reach the final value. A real time of 2 to 2.5 second was required in order to determining a single operating point.

4.6.2 Results

The steady state results obtained from the computer model was compared with a practical brushless excitation system at Haripur power station of BPDB. The exciter response at different terminal voltages were available. From a case study, the results at 0.9 pu of voltage were chosen for comparasion. The test results for Haripur system is presented in figure 4.5a And the

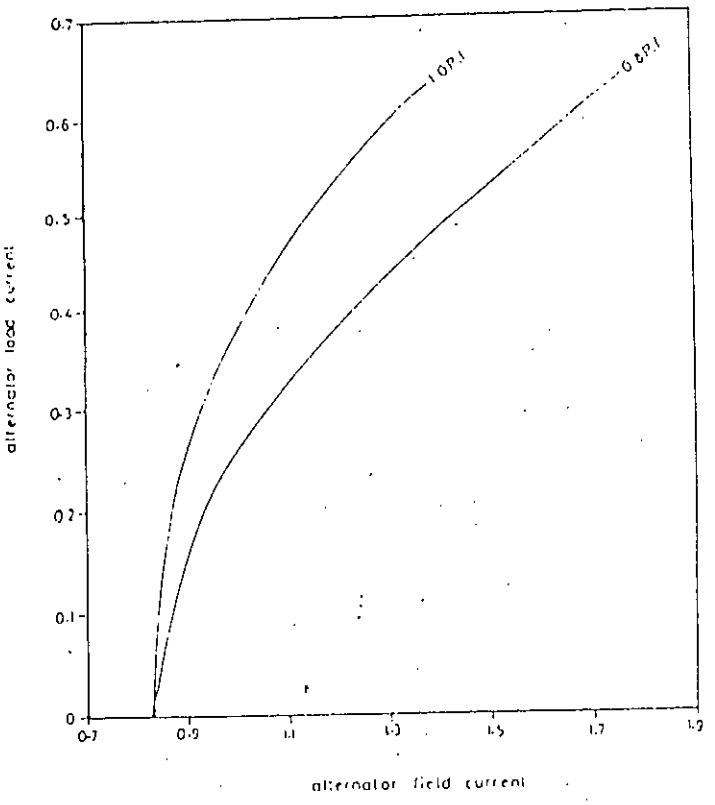

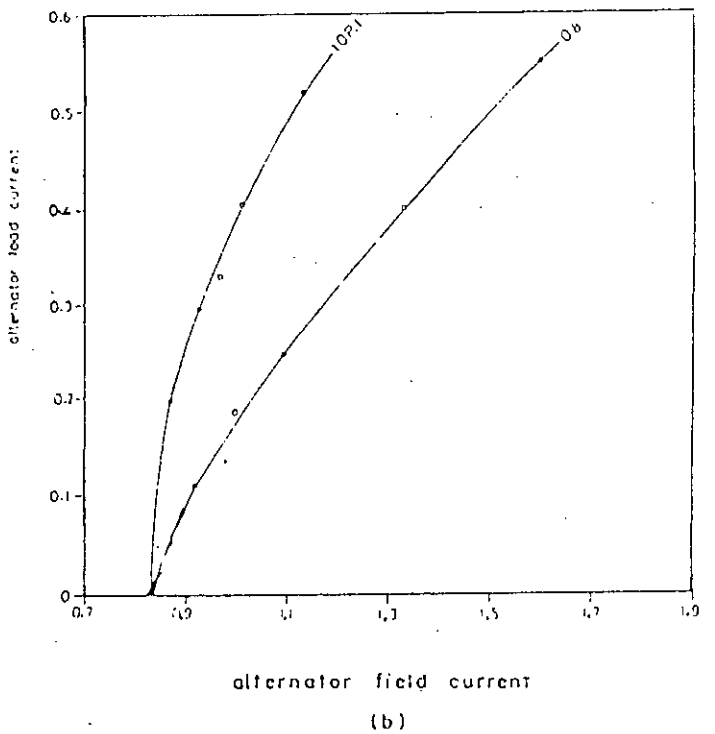

Fig. 4.5 Steady state characteristics curve

(a) Real system

(b) Computed system

computed results are shown in figure 4.5b. The two figure compares well. The slight deviation was due to inavailability of data of the practical system. The shape of the curves indicates that the model's prediction of the steady state responses are equally good.

Chapter 5

CONCLUSIONS AND DISCUSSIONS

5.1 Conclusion and discussions

A model for brushless excitation system of an alternator has been developed. The model was based on the mathematical analysis of the excitation system. A brushless excitation system supplies the dc output power to the field of an alternator through a rectification process and the operation of the system mainly depends on the mode of operations of the rectifier unit. The rectifier undergoes four distinct mode of operations as its output current and/or input voltages vary. In this study, Both analytical and graphical explanation of each mode of operation have been presented. A particular mode of operation is distinguished from the value of normalised current, I_n which is a function of output current, input voltage and machine's commutating reactance X_c. From the knowledge of operating mode the dc output voltage applied across field winding is determined by calculating the loading factor, F_{ex} which is again obtainable from the regulation curve relating F_{ex} and I_n.

The model developed can be applied to simulate a range of transient involving switching operation, which are common in a power system. The transient model incorporated the exciter-alternator, rectifier, main alternator and load. The alternator models were simulated on the basis of machine's two axis theory. The machine models were simplified by neglecting the stator dc

component which greatly reduces the computation time. The output current of the rectifier constitutes the field current of the main alternator which is fedback as exciter's alternator stator current. The feedback is accomplished by resolving the d.c. output current, first, in real and reactive components and then into direct and quadrature axis components. The effect of delay angle on the two axis currents is also taken into account in the present analysis.

The model was compared with test results and found to agree well. Its accuracy against IEEE model was also shown. Oversimplification and non-existent of effect of delay angle on the current resolution are found to be the main reasons behind the inaccuracy of IEEE model.

The transient model was also used to simulate the steady state responses of a brushless exciter model. They were compared with similar responses of a practical system supplied by manufacturer. The outcome of the developed model was found to be satisfactory.

The present work has contributed towards a long-awaited need for an accurate model of brushless excitation system. The model evolved from the study can be used in multi-machine power system analysis.

5.2 Further works

This study has created scope for research in new areas on brushless excitation system. Some of them are summerised below:

(a) The steady state responses in this study were calculated indirectly by running the transient model for short duration of time. But practically a solution technique should be developed in order to evaluate the steady state quantities directly. The work on steady state should receive immediate attention, because this study is very important in day-to-day affairs.

(b) The exciter model used in this study was a direct one. In practice, exciter is always provided in conjunction with automatic voltage regualtor (AVR). A study should be carried out in order to incorporate AVR model and the observer, the effect of AVR on exciter response.

(c) Since a machine is a component of multi-machine power system. Techniques of inclusion of brushless excitation system representation in multimachine system modelling should be formulated. The study requires defining exciter's quantities in the combined d-q frame of reference. The differential equations within the model is solved using Runge-Kutta routine, but for multimachine study, the routine should be replaced by any other faster one in order to reduce the computation time.

REFERENCES

1. E. W. Kimberk :"Power System Stability, Vol.3, a book published by Wiley, NewYork, 1956.

2. O. W. Hanson, C. T. Goodwin, and P. L. Dandeno : "Influence of excitation and speed control parameters in stabilizing intersystem oscillations" IEEE Transaction on power apparatus and systems, Vol PAS-87, 1968, pp 1306-13.

3. C. Concordia : "Synchrnous Wachines" , a book published by John Wiley and Sons, Newyork, 1951, pp 216-219.

4. M. Temoshok and F.S. Rothe : "Excitation voltage response defination and significance in power systems" AIEE Trans. PAS-76, 1957, pp 1491-96.

5. C. Concordia : "Effect of boost-back voltage regulator on steady-state power limit" AIEE Trans. PAS-69, 1950. pp 380-84.

6. Westinghouse Electric Corporation: "Electrical Transmission and Distribution Reference Book." Pittsburgh, Pa ., 1950.

7. H. A. Cornetius, W. F. Cawson and H. W. Cory: "Experience with automatic voltage regulation on a 115-megawatt turbo-generator." AIEE Trans. PAS-71, 1952, pp 184-87.

8. H. C. Barnes, J.A. Oliver, S.A. Rubenstein and M. Temoshok : "Alternator-rectifier exciter for cardinal plant" IEEE Trans. PAS-87, 1968, pp 1189-98.

9. Whitney, E.C., Hoover, D.B. and Bobo, P.O.: "An electric utility brushless excitation system" AIEE Trans, PAS -78, 1959, pp 1821-24.

10. P. O. Bobo,J. T. Carlson, and J. F. Horton: "A new regulator and excitation system" IEEE Trans. PAS-72, 1953, pp 172-83.

11. H.W. Gayek: "Transfer Characteristics of Brushless Aircraft Generator Systems", IEEE Transactions on Aerospace, Vol.2, No. 2, April 1964. pp 913-928.

12. L.M. Domeratzky, A,S. Rubenstein and M. Temoshok : "A static excitation system for industrial and utility steam-turbine generators" AIEE Trans. PAS-80, 1961, pp 1072-77.

13. L.J. Lane, D.F. Rogers and P.A. Vane "Design and tests of a static excitation system for industrial and utility steam-turbine generators" AIEE Trans. PAS-80, 1961, pp 1077-85.

14. R.L. Witzke, J.V. Kresser and J.K. Dillard, :"Influence of AC Reactance on Voltage Regulation of 6-phase Rectifiers" AIEE Transactions, Vol. 72, July, 1953, pp 244-253.

15. E.F. Christensen, C.H. Willis and C.C. Herskind : "Analysis of Rectifier Circuits", AIEE Transactions, Volume 63, 1944, pp 1048-58.

16. A.F. Puchstein, T.C. Lloyd and A.G. Conrad "Alternating current Machines", A book published by John Wiley and Sons, Inc., New York, 3rd edition, 1954.

17. R.W. Ferguson, H. Herbst, R.W. Miller: "Analytical Studies of the Brushless Excitation System", AIEE Transactions, Part III(B), Vol. 78, February, 1960, pp 1815-1821.

18. W.J. Shilling "Exciter armature reaction and excitation requirements in a brushless rotating rectifier aircraft alternator" AEEE Transaction Part II(Applications & industry), Vol. 79, Nov. 1960, pp 394-402.

19. IEEE Committee Report: "Computer Representation of Excitation Systems" IEEE Transactions on Power Apparatus and Systems, Vol. PAS-87, June 1968, pp 1460-1464.

20. IEEE Committee Report: "Excitation System models for Power System stability Studies" IEEE Transactions on Power Apparatus and Systems, Vol. PAS-100, 1981, pp 494-509.

21. D.O' Kelly and S. Simons: "Introduction to Generalised Electrical Machine Theory" A book published by McGraw Hill and Co., Great Britain. 1968.

22. I.M. Canay "Determination of model parameters of synchronous machines" IEE procedings, Vol. 130, pt B, No.2, March 1983, pp 86-94.

23. Shackshaft, G. : "New approach to the determination of Synchronous machines parameters from tests. "Proc. IEE, Vol. 121, No.11, November, 1974, pp 1385-1392.

24. Takeda, Y. and Adkins, B: "Determination of synchronous machine parameters allowing for unequal mutual inductances." Proc. IEE Vol. 121, No. 12, December, 1974, pp 1501-1504.

25. Dandeno, P.L. and Poray, A.T. : "Development of detailed turbogenerator equivalent circuits from standstill frequency response measurement" IEEE Transactions on Power Apparatus and System, Vol. PAS-100, No.4, April 1981, pp 1646-1655.

26. S.M.L. Kabir "Computer modelling of large turbine alternators" Ph.D. Thesis, University of Manchester, 1989.

27. B. Adkins and R. Harlay: "The General Theory of Alternating Current Machines" A book published by Chapman and Hall, London.

28. H.W. Gayek "Behaviour of brushless aircraft generating system" IEEE Transactions on Aerospace, Vol. AS-1, No. 2, August, 1963, pp. 594-622.

29. D.W. Auckland, R. Shulttleworth "Micromachine model of brushless excitation System" A report submitted to G.E.C turbine-generators Ltd. Stafford, England, 1990.